



## Damaging and protective interactions of lichens and biofilms on ceramic *dolia* and sculptures of the International Museum of Ceramics, Faenza, Italy



Daniela Pinna<sup>a,\*</sup>, Valentina Mazzotti<sup>b</sup>, Sabrina Gualtieri<sup>c</sup>, Samuele Voyron<sup>d</sup>, Alessia Andreotti<sup>e</sup>, Sergio Enrico Favero-Longo<sup>d</sup>

<sup>a</sup> Chemistry Department, University of Bologna, Ravenna Campus, via Guaccimanni 42, Ravenna, Italy

<sup>b</sup> Museo Internazionale delle Ceramiche in Faenza, Viale Baccarini 19, 48018 Faenza, RA, Italy

<sup>c</sup> Institute of Science and Technology for Ceramics, National Research Council, Via Granarolo 64, 48018 Faenza, RA, Italy

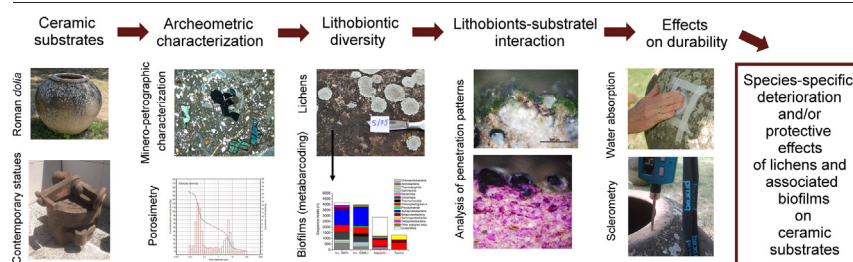
<sup>d</sup> Dipartimento di Scienze della Vita e Biologia dei Sistemi (Life Sciences and Systems Biology), viale Mattioli 25, 10125 Torino, Italy

<sup>e</sup> Department of Chemistry and Industrial Chemistry, University of Pisa, via Moruzzi 13, Pisa, Italy

### HIGHLIGHTS

- Lichen and microbial diversity on ceramics with different composition and porosity
- Biodeterioration and bioprotection effects of lithobionts colonizing ceramics
- Black fungi on and beneath the lichens *Acarospora gallica* and *Verrucaria nigrescens*
- Interactions between lichens and ceramics affecting surface hardness
- Lichens reduce the amount of absorbed water limiting the water ingress.

### GRAPHICAL ABSTRACT



### ARTICLE INFO

Editor: Patricia Sanmartin

#### Keywords:

Outdoor ceramic artworks  
Archaeometry  
Porosity  
Lithobionts  
Biodeterioration  
Bioprotection  
Black meristematic fungi  
Bioreceptivity  
Metabarcoding

### ABSTRACT

Although ceramic objects are an important part of the worldwide cultural heritage, few investigations on the effects of lithobiontic growth on their outdoor conservation are available in the literature. Many aspects of the interaction between lithobionts and stones are still unknown or strongly debated, as in the case of equilibria between biodeterioration and bioprotection. This paper describes research on the colonization by lithobionts on outdoor ceramic Roman *dolia* and contemporary sculptures of the International Museum of Ceramics, Faenza (Italy). Accordingly, the study i) characterized the mineralogical composition and petrographic structure of the artworks, ii) performed porosimetric measurements, iii) identified lichen and microbial diversity, iv) elucidated the interaction of the lithobionts with the substrates. Moreover, v) the measurements of variability in stone surface hardness and in water absorption of colonized and uncolonized areas were collected to assess damaging and/or protective effects by the lithobionts. The investigation showed how the biological colonization depends on physical properties of the substrates as well on climatic conditions of environments in which the ceramic artworks are located. The results indicated that lichens *Protoparmeliopsis muralis* and *Lecanora campestris* may have a bioprotective effect on ceramics with high total porosity and pores with very small diameters, as they poorly penetrate the substrate, do not negatively affect surface hardness and are able to reduce the amount of absorbed water limiting the water ingress. By contrast, *Verrucaria nigrescens*, here widely found in association with rock-dwelling fungi, deeply penetrate terracotta causing substrate disaggregation, with negative consequences on surface hardness and water absorption. Accordingly, a careful evaluation of the

\* Corresponding author.

E-mail addresses: [daniela.pinna@outlook.com](mailto:daniela.pinna@outlook.com) (D. Pinna), [valentinamazotti@micfaenza.org](mailto:valentinamazotti@micfaenza.org) (V. Mazzotti), [sabrina.gualtieri@issmc.cnr.it](mailto:sabrina.gualtieri@issmc.cnr.it) (S. Gualtieri), [samuele.voyron@unito.it](mailto:samuele.voyron@unito.it) (S. Voyron), [alessia.andreotti@unipi.it](mailto:alessia.andreotti@unipi.it) (A. Andreotti), [sergio.favero@unito.it](mailto:sergio.favero@unito.it) (S.E. Favero-Longo).

<http://dx.doi.org/10.1016/j.scitotenv.2023.162607>

Received 25 October 2022; Received in revised form 24 February 2023; Accepted 28 February 2023

Available online 10 March 2023

0048-9697/© 2023 The Authors. Published by Elsevier B.V. This is an open access article under the CC BY license (<http://creativecommons.org/licenses/by/4.0/>).

negative and positive effects of lichens must be carried out before deciding their removal. Regarding biofilms, their barrier efficacy is related to their thickness and composition. Even if thin, they can impact negatively on substrates enhancing the water absorption in comparison to uncolonized parts.

## 1. Introduction

The occurrence of rock-dwelling organisms - called lithobionts - on outdoor stone artworks is well-known and has been described in many papers so far (Favero-Longo and Viles, 2020; Pinna, 2021). Although bare and exposed rock surfaces are considered an extreme habitat characterized by intense fluctuations in light, temperature, and hydration, lithobionts, such as lichens and biofilm-forming microorganisms, have developed a variety of strategies to endure such conditions (Gorbushina and Broughton, 2009; Spribille et al., 2022). Lichens have been recently redefined as self-sustaining ecosystems formed by the interaction of an exhabitant fungus (mycobiont), an extracellular arrangement of one or more photosynthetic partners (green algal and/or cyanobacterial photobiont(s)) and an indeterminate number of other microscopic organisms (the lichen microbiome, mostly including bacteria and additional fungi) (Hawksworth and Grube, 2020). Multiple genotypes of all these different partners can occur in a single symbiotic thallus, but it generally appears as a visually distinct, structured individual, which is the symbiotic phenotype of the primary fungal partner, of which it bears the name (Honegger, 2012; Allen and Lendemer, 2022). Biofilms are aggregations of microorganisms (bacteria, algae, fungi, protozoa) and their extracellular products (extra cellular polymeric substances - EPS, also called extracellular matrix - ECM), which keep the cells physically and functionally together and attached to a surface, giving rise to a supracellular organization (Flemming et al., 2007, 2016). Although there are similarities between lichens and biofilms, including the binding of their structures by EPS (Carr et al., 2021), the prominence of the primary fungal partners in the structural and functional control of the symbiotic consortia of lichens, reflected in their systematic placement in Kingdom Fungi, make them biological entities different from microbial biofilms.

Lithobionts interact either with each other forming complex communities or with the rock substrate. The rock surface habitat includes various differentiated microhabitats. Epilithic organisms thrive predominantly on the surface and a minor component of the biomass or of the thallus develops inside the rock, while endolithic organisms live just beneath the surface using a thin layer of the rock surface for protection against the environmental adverse conditions (e.g., light protection and storage of water) (Omelon, 2016).

Subjects related with colonization by microorganisms and lichens on stone artworks are biodiversity, deteriorative or negligible effects, protection, esthetical disfigurements, chromatic alterations, control and preventive actions. Understanding of the effects of lichen and microbial development on stones is essential to plan appropriate conservation procedures (Favero-Longo and Viles, 2020; Pinna, 2021).

Like natural rock outcrops, stone artworks differ in surface texture, hardness, porosity, pH and chemical composition, i.e. characteristics that make them favorable or unfavorable to microbial colonization. The susceptibility of stone materials to hold organisms is called bioreceptivity, a term coined by Olivier Guillitte (Guillitte, 1995), which, in other words, indicates the aptitude of a stone to be vulnerable to organisms' colonization. According to Guillitte's further definition of this concept, the primary bioreceptivity is the potential of a healthy material to be colonized; the secondary bioreceptivity is the condition of a material deteriorated by abiotic and biotic factors; finally, the tertiary bioreceptivity is the condition of a material affected by human activities (e.g., application of water repellents and consolidants, biocides, etc.). Sanmartín et al. (2021) have recently proposed to split Guillitte's tertiary bioreceptivity into two, with tertiary bioreceptivity used for human actions that cause physical changes to the materials (for instance the use of mechanical and laser methods), and

quaternary bioreceptivity when new materials, as coatings or chemicals that can leave residues, are added to stones.

At present, many relevant studies have documented and discussed the interaction between biological growths and cultural heritage, and the importance of mechanical/physical and chemical biodeterioration processes and their negative effects on the durability on historical objects of art has reached growing attention of professionals in charge of the conservation management (among others Seaward, 1997; de los Rios et al., 2009; Sterflinger, 2010; Favero-Longo et al., 2011; Miller et al., 2012; Onofri et al., 2014; Salvadori and Casanova, 2016; Morando et al., 2017; Urzì et al., 2018). However, despite considerable research efforts, there are still general issues that need to be addressed. Many aspects of the interaction between microbial communities, lichens and stone materials are still unknown. Not surprisingly, in recent times many papers have reported that the homogeneous and widespread colonization of outdoor stones, rather than exerting biodeterioration, may act as a protective layer shielding the materials from other factors that cause decay, such as wind and rainwater (Pinna, 2014; Liu et al., 2020). In particular, bioprotection may derive from a passive action of the lithobionts, with their biomass providing an umbrella-like effect, or from an active consolidation of the mineral surfaces by dissolution-reprecipitation, and biomineralization processes (Naylor et al., 2002; Carter and Viles, 2005; Liu et al., 2022). Remarkably, biodeterioration and bioprotection processes do not necessarily result mutually exclusive and may be contemporarily activated by a specific lithobiont on a lithic substrate. The final effect of stone surface durability derives from the balance between the two contrasting processes under a specific (micro-)climate condition (Bungartz et al., 2004; Carter and Viles, 2005; McIlroy de la Rosa et al., 2013). However, information on such equilibria and their consequent effects on stone conservation is still limited to few case studies, representative of a limited number of lithobionts, lithologies and environmental conditions, so that further investigations are still needed.

Studies on lichen and biofilm interactions with stone materials have been performed mainly on granites, sandstones, marbles, and other calcareous lithologies. Lesser investigations are available on ceramic objects although they are an important part of the worldwide cultural heritage (Pena-Poza et al., 2018; Quagliarini et al., 2019; Guiamet et al., 2019; review in Fomina and Skorochood, 2020). Bioreceptivity of ceramics mainly relates to physical characteristics such as porosity and surface roughness (Gazulla et al., 2011; Coutinho et al., 2015). *In vitro* tests performed inoculating microbial communities, isolated from outdoor artworks, on ceramic roofing tiles demonstrated that these substrates are highly bioreceptive to microbial colonization (Laiz et al., 2006). The smooth and impermeable surface of glazes is more resistant to microbial colonization. The results available for lichens, mostly dealing with bricks and ceramic roofing tiles, generally displayed biogeochemical interaction patterns yielding biodeterioration effects (Radeka et al., 2007), and the physical detachment of mineral layers has been also documented (Seaward, 2004; Guiamet et al., 2019).

This study focused on outdoor ceramic Roman *dolia* and contemporary sculptures of the International Museum of Ceramics (MIC), Faenza (Italy), and included aspects of their production and state of conservation connected to the biological colonization by lichens, a black fungal biofilm overgrowing lichens and other biofilms. It aimed at verifying the hypothesis that the interactions of lithobionts with the ceramics may positively affect physical properties related to surface durability, namely water absorption and surface hardness. Thus, microscopic samples of the ceramic substrates were taken to perform archaeometric investigations, including the characterization of the mineralogical composition and petrographic structure,

and to carry out porosimetry measurements. Lichen and microbial diversity on the ceramic surfaces were characterized by direct and microscopic observations, and by metabarcoding analyses. The interaction of lithobionts with the substrates was elucidated by microscopic methods. The variability in stone surface hardness and the water absorption of colonized and uncolonized areas were quantified by sclerometric measures and the sponge method, respectively, to better illustrate and highlight any protective effects generated by the biological colonization. Analyses performed on each of the seven artworks are summarized in Table S1. The information collected has provided indications for the definition of the restoration project.

## 2. Materials and methods

### 2.1. The artworks selected for the study and the climatic survey

The MIC is located in Faenza (latitude 44°28'33" N, longitude 11°88'33" E, 36 m at sea level), a town of the SE part of the Po Plain, which is characterized by the sub-Mediterranean variant of the temperate macrobioclimate (Pesaresi et al., 2017). Air temperatures range from av. 6 °C in winter to av. 24 °C in summer, and RH values from av. 75 % in winter to av. 56 % in summer (dataset 2011–2021, obtained by the Osservatorio Meteorologico Torricelli - a civic institution specialized in meteorology, based in Faenza and not far from the MIC). Table S2 shows the yearly average values of temperature (min and max) and annual precipitation in the period 2011–2021.

Five Roman terracotta *dolia* are in the internal garden of the MIC (Fig. 1a). Four are in contact with the ground and grass while one is placed on a brick base. The bigger one (inventory n. 10366,1 h 165 × Ø 120 cm) comes from Giarre (Sicily) where it was purchased in 1940 for the MIC by Domenico Rambelli, a distinguished artist and teacher at the Royal School of Ceramics of Faenza. The *dolium* was housed indoors until 1950. The other four *dolia* (inventory n. 19074-19077, respectively h 77 × Ø 84 cm, h 83 × Ø 84 cm, h 57 × Ø 61 cm, h 44,5 × Ø 46,5 cm) are smaller than the great one. They come from San Paolo in Civitate (the ancient *Teanum Apulum*) in Puglia, where they were found in the 1960s and donated to the MIC by Germano Belletti in 1978. Their location in the museum's garden dates to the second half of the eighties. The top openings of all *dolia* are covered with an iron cap.

Other ceramic objects have been included in this study, that are two contemporary sculptures located on a tiled terrace of the MIC, namely



Fig. 1. Ceramic artworks at the International Museum of Ceramics (MIC). a) Roman *dolia* located in the internal garden of the MIC. The inventory numbers are indicated; sculptures b) *Volumes* by Vladimir Tsivin and c) *Big machine that grinds* by Romano Mazzini located in the terrace of the MIC.

“*Volumes*” by Vladimir Tsivin (made in 1982, inventory n. 20807 h 68 × 120 × 50 cm) (Fig. 1b) and “*Big machine that grinds*” by Romano Mazzini (made in 1992, inventory n. F283 h 98 × 110 × 102 cm) (Fig. 1c). Tsivin's work is a refractory ceramic, while Mazzini's sculpture is a semi-refractory slipped earthenware. Both works have been exhibited outdoors since 2010.

Temperature (T) and relative humidity (RH) were monitored in the garden (July 27–November 13/2021, and February–June/2022) and in the terrace (July 27/2021–January 26/2022, and February–June 2022) using Tinytag TGU-4500 sensors (Gemini Data Loggers).

The state of conservation of the *dolia* is affected by a widespread biological colonization, as well as by abiotic deterioration of the terracotta, combined with efflorescence, in some areas. A preliminary diagnostic investigation had been conducted for the characterization of the degradation patterns (Mazzotti et al., 2021). The state of conservation of the two sculptures instead has not been investigated so far.

### 2.2. Mineralogical and petrographic investigations

All the *dolia* and the sculptures were investigated. Some small samples of the ceramic materials were collected from the inner surface of the *dolia*, when possible, and from preexisting lacunae of both *dolia* and sculptures, by using a scalpel. Multiple methodologies such as optical microscopy on thin sections (OM), X-ray powder diffraction (XRPD) and energy-dispersion X-Ray fluorescence (XRF-EDS) were conducted.

The microstructure, the mineralogical composition, and the deterioration forms (when present) were observed on thin sections by optical microscopy under transmitted polarized light (PLM, Olympus BX51).

XRF-EDS was used to determine the chemical composition of ceramic bodies. The X-ray spectrometer S2 PUMA (Bruker) was employed setting the following working conditions: palladium tube power 4 kW, power generator 50KV. The analysis was performed on a glass disk (diameter 40 mm; analysis area 37 mm) obtained by melting 1 g of sample powder mixed with 9 g of melting mixture (lithium meta- and tetraborate) and 3 drops of lithium iodide. A Claisse Fluxer 10 was used to reach a melting temperature of 1150 °C. The analysis was performed by using a calibrated program specific for ceramics. The chemical composition is reported as weight percent oxides.

Qualitative mineralogical analyses of powdered samples (XRPD-X-ray Powder Diffraction) were obtained with a Bruker D8 Advance X-ray diffractometer equipped with the LynxEye detector; the data were collected in the range 4–64 2θ with a step-size of 0.020° and a scan velocity 1°/min in low background conditions. The interpretation of the diffraction patterns was made by using as reference the ICDD (International Centre for Diffraction Data) database (XRD 2022 PDF® Database Products).

### 2.3. Pyrolysis gas chromatography–mass spectrometry (Py-GC–MS)

The Py-GC–MS analysis was performed on a sample (around 5 mm<sup>3</sup>) from the sculpture “*Volumes*” to better characterize its composition. We selected only this sculpture because it had a colonization very different from the *dolia* and the other sculpture. We wanted to go into the details of its composition to understand if it was a cause, among others, of the diverse colonization. The instrumentation consisted of a micro-furnace Multi-Shot Pyrolyzer EGA/Py-3030D (Frontier Lab) coupled with a gas chromatograph 6890 Agilent Technologies (Palo Alto, USA) equipped with split/spitless injector. The GC was coupled with a 5973 Agilent Mass Selective Detector (Palo Alto, USA) single quadrupole mass. The pyrolysis temperature was 550 °C with the Py-GC interface at 180 °C. The sample was inserted in the stainless-steel cup and then into the micro-furnace. Pyrolysis was performed both without and with 5 µl of 1,1,1,3,3,3-hexamethyldisilazane (HMDS, chemical purity 99.9 %, Sigma Aldrich Inc., USA), as silylation agent for the in situ thermally assisted derivatization of pyrolysis products, to replace hydroxylic and carboxylic hydrogens with trimethyl silyl groups. Chromatographic separation was performed on a fused silica capillary column HP-5MS (stationary phase 5 % diphenyl- 95 % dimethylpolysiloxane,

30 m length  $\times$  0.25 mm inner diameter, Hewlett Packard, USA) with a deactivated silica pre-column (2 m  $\times$  0.32 mm i.d., Agilent J&W, USA). Chromatographic conditions were as follows: initial temperature 36 °C, 2 min isothermal, 10 °C/min up to 300 °C, and 30 min isothermal. The carrier gas was helium (99.9995 % pure), the flow was 1.0 ml/min and the split ratio 1:10. The analytical procedure is reported in Bonaduce and Andreotti (2009).

#### 2.4. Porosimetry measurements

Porosimetry measurements were carried out to characterize the total open porosity and the pore size distribution of the ceramic body of the *dolia* and the sculptures. A very small fragment from each artwork (around 1 cm<sup>3</sup>) was analyzed by using PASCAL 240/140 Mercury porosimeter (Pascal 240 measures pore size diameter in the range 10,000 and 8-10 nm, and Pascal 140 measures pore size diameter in the range 100–3.5  $\mu$ m). Since mercury is a non-wetting liquid, it does not spontaneously penetrate pores by capillary action, but must be forced by external pressure. The required pressure is inversely proportional to the size of the pores. Mercury fills the larger pores first and, as pressure increases, the smaller ones. The volume and size distributions are determined according to the Washburn equation. This investigation provided the pores size distribution, the percentages amounts of small and big pores and the value of total open porosity. The observations of thin sections under the optical microscope added information about objects' porosity.

#### 2.5. Survey and sampling of biofilms and lichens and investigations by optical microscopy

The biological colonization was firstly assessed through naked eye observation and then was observed under a hand lens (9 $\times$  magnification). On each *dolium*, a survey of the percentage coverage of different lithobiontic components (lichens, biofilms, mosses), and of specific lichen diversity, was conducted. In particular, per each *dolium*, couple of plots (h  $\times$  l: 10  $\times$  5 cm) were established on surfaces displaying different inclinations (between 30° and 155°) on the left and the right of the North- and South-facing axes at 3–7 different distances between the opening and the ground depending on the *dolium* size (number of plots:  $n = 10$  on inv. 19074 and 19075,  $n = 8$  on inv. 19076;  $n = 6$  on inv. 19,077;  $n = 14$  on inv. 10366,1). Six plots were also distributed on horizontal, sloped and vertical surfaces of Mazzini's sculpture.

Microsamples of lichens and biofilms were collected from the *dolia* and the sculptures and observed with a Zeiss Stemi 2000-C stereomicroscope and a Nikon Eclipse 50i microscope. Lichens were identified with standard methodologies (microscopy study of morphological and anatomical characters, color spot tests), using Clauzade and Roux (1985) and the online keys published in Italic, the Information System of the Italian Lichens (see Nimis and Martellos, 2020), accessed in the period May–July 2021 and January 2023. Nomenclature follows Nimis (2016); ecological indicator values for each species (pH, pH of the substratum; SI, solar irradiation; AR, aridity; EU, eutrophication; PO, poleotolerance) are reported following Nimis (2022).

A preliminary characterization of the biofilm-forming microorganisms was performed observing their morphological and anatomical features with the optical microscope Zeiss Axioplan 2, thereafter supported with metabarcoding analyses (see below).

Fragments of substrates colonized by biofilms and lichens were taken with the aid of a lancet and used to i) perform the metabarcoding analyses and ii) investigate the lithobionts-rock interaction. Both the number and the dimension of the samples were limited for conservative reasons. It was not possible to take samples of all lichens because the configuration of the objects did not allow it. Fragments of the samples were embedded in epoxy resin, dry-ground and polished. The cross sections were examined at the microscope Zeiss Axioscop, which features a halogen bulb and a mercury lamp for visible and ultraviolet illuminations, respectively, and is equipped with a video camera. Some cross sections were stained with

Periodic Acid Schiff (PAS, Sigma Aldrich, St. Louis, MO, USA), according to Whitlatch and Johnson (1974). PAS allows to visualize the biological component within the lithic substrate since it stains carbohydrates. It is used to detect cells as well as extracellular polymeric substances (EPS) on/inside rocks. Six lichens and microorganisms' cross sections were stained, namely, *Lecidea fuscoatra* ( $n = 1$ ), *Protoparmeliopsis muralis* (1), *Lecanora campestris* (1), *Verrucaria nigrescens* (1) and a black-gray layer of fungal biofilm overgrowing *V. nigrescens* (2). They were selected for their wide distribution on the surfaces.

#### 2.6. Metabarcoding analysis

Metabarcoding analyses were performed on black-gray layers of fungal biofilm overgrowing lichens scraped from two *dolia* (surfaces of inv. 10366,1 and 19074, selected as representative of this prominent microbial phenomenology) and Mazzini's sculpture, and on a biofilm from Tsvini's sculpture. The total DNA was extracted from 30 mg of scraped material by means of the DNeasy Plant Pro Kit (Qiagen, Milano, Italy) following the manufacturer's instructions. The obtained DNA was quantified by means of the NanoDrop 1000 Spectrophotometer (Thermo Fisher Scientific, Milano, Italy). In order to evaluate the microbial communities, targeted metabarcoding profiling of the samples was carried out by sequencing the rDNA ITS2 region of fungi and V3–V4 region of rDNA 16S of prokaryotes. More in detail, 20 ng per sample of DNA were amplified using the primer sets fITS9-ITS4 (White et al., 1990; Ihrmark et al., 2012) and pro341f-806rB (Takahashi et al., 2014; Apprill et al., 2015) for fungi and prokaryotes, respectively. The two primer sets were added with the following Illumina overhang adapter sequences: forward overhang, 5'-TCGT CGGCAGCGTCAGATGTGTATAAGAGACAG-[locus specific target primer], reverse overhang, 5'-GTCTCGTGGCTCGGAGATGTGTATAAGAGACAG-[locus specific target primer]. The PCR conditions for fungi were: an initial step at 95 °C for 15 min, 27 cycles at 95 °C for 30 s, 57 °C for 30 s, 72 °C for 30 s, and a final extension step of 72 °C for 7 min. The conditions for prokaryotes were: an initial step at 94 °C for 3 min, 30 cycles at 94 °C for 45 s, 57 °C for 45 s, 72 °C for 60 s and a final extension step of 72 °C for 10 min. For all specimens, DNA extracted was amplified in triplicate and pooled prior to the purification by means of the Wizard® SV Gel and PCR Clean-Up System (Promega). Purified products were quantified with Qubit dsDNA BR Assay kit and Qubit Fluorometer 2.0 (Thermo Fisher Scientific, Milano, Italy) following the manufacturer's protocol and sent for Illumina MiSeq sequencing (2  $\times$  250 bp) to IGA technologies (Udine, Italy).

#### 2.7. Bioinformatic and data analysis

For each sample, DNA raw reads included forward and reverse sequences in separate files. Sequencing adapters and primers were then removed, and the sequences were analyzed using the bioinformatics platform QIIME2 (Quantitative Insights Into Microbial Ecology 2, version 2019.7; Bolyen et al., 2019). The DADA2 plugin (Callahan et al., 2016) was used for quality control, the denoising and the removal of chimeric sequences. The taxonomic assignment was achieved using as reference database the UNITE QIIME release for fungi version 10.05.2021 (Abarenkov et al., 2021) and Greengenes 13.8 99 % OTUs full-length sequences (Robeson et al., 2021, Bokulich et al., 2018) for prokaryotes. The datasets generated for this study can be found in the NCBI Sequence Read Archive (SRA-NCBI; <https://www.ncbi.nlm.nih.gov/sra>) under project accession numbers (PRJNA850120; PRJNA850127).

#### 2.8. Sclerometric measurements

Variability in stone surface hardness was measured using an Equotip Piccolo 2, DL-type (Proceq, Switzerland), a rock surface hardness rebound device ideal for use on soft and weathered surfaces (Morando et al., 2017). In brief, the DL probe, that is a 2.78 mm diameter spherical tungsten carbide test tip, impacts at 11.1 N mm against the test surface. The ratio

between the velocity after and before impact ( $V_2/V_1 \times 1000$ ) is measured and expressed by the Leeb Hardness (HL) unit.

The measures were performed in areas of two *dolia* (inv. 19074 and 19075) colonized by the lichens *Protoparmeliopsis muralis* and *Verrucaria nigrescens*, and in uncolonized parts, which were all localized above the major curvature, near the edges of the openings. The two lichen species were selected for their high frequency and cover, and the *dolia* were selected because the two species were widespread on their surfaces. The thalli were gently removed with a scalpel and 9 micro-areas corresponding to the substrate beneath the lichens and to the uncolonized terracotta were selected. Following the Simple Impact Method (SIM; Wilhelm et al., 2016), fifteen measures were carried out on each of the 27 micro-areas to evaluate the rock hardness of surface and subsurface of the colonized and uncolonized substrate. Data were visualized as boxplots obtained using Origin (Pro), Version 2021 (OriginLab Corporation, Northampton, MA, USA); significant differences between colonized and uncolonized parts were evaluated by ANOVA with post-hoc Tukey's test using Systat 10.2 (SYSTAT, Evanston, IL, USA).

### 2.9. Water absorption by contact sponge method

The measurements of water absorption on different lithobiontic components (lichens and biofilms) and on uncolonized areas were performed on three *dolia*, selected as representative of the main colonization patterns observed on the five *dolia*, in different meteorological seasons. In particular, the measurements on lichens were carried out on areas mostly colonized by *L. campestris* and *P. muralis* (inv. 19074 and 19075) and *L. gr. fuscoatra* (inv. 10366,1), while those on biofilms dealt with the black-gray layer of fungal biofilm overgrowing *V. nigrescens* (inv. 19074 and 19075) and a green and black biofilm (inv. 10366,1). The analysis was not applied on the two sculptures because the colonization pattern and the ceramics were different.

Surfaces colonized by lichens and biofilms were compared to uncolonized surfaces to assess their differences in water absorption and evaluate a potential barrier-effect of the biological component.

A set of measurements was repeated on parcels of *dolia* inv. 19074 and 19075 from which the lithobiontic components had been mechanically removed with a lancet. Such measurements did not provide information about the effect of lithobionts when they are anchored to the terracotta surface, but about the substrate conditions once they naturally decay or are removed by restorers.

The measurements were performed in December 2020, May and October 2021, and, after the removal of lithobionts, in December 2022 using the contact sponge method that has been standardized by the European Committee for Standardization (EN 17655, 2021). It consists of a 1034 Rodac plate (5.6 cm in diameter) containing a natural fiber Calypso sponge by Spontex that was imbibed with approximately 5 ml of distilled water. This makes the sponge thicker than the rim of the plate. The plate was pressed on the stone surfaces for 30 s. Nine spot measurements for each *dolium* were carried out *in situ* on selected zones (three spots with lichens, three spots with biofilms, and three uncolonized spots). Water absorption was determined by calculating the difference, in  $\text{mg}/\text{cm}^2$ , between the plate weights measured before and after contact with the surfaces. Specific morphologies of the biological colonization and the uncolonized zones were taken as reference points of sponge reposition.

Formula (1) calculates water absorption per square centimeter and unit of time.

$$W_a (\text{mg}/\text{cm}^2 \text{ min}) = m_i - m_f / A t \quad (1)$$

where

- $m_i$  initial weight of the sponge inside the plate (mg)
- $m_f$  weight of the sponge inside the plate after contact (mg)
- A sponge area ( $0.2376 \text{ cm}^2$ )
- t time (0.5 min)

Generalized Linear Model (GLM) was applied to evaluate the influence of the different substrates (each *dolium*), lithobiontic colonization (lichen, biofilm, uncolonized), and measurement period (winter, spring, autumn) on the water absorption before the removal of lithobionts. In particular, a factorial ANOVA was carried out by SYSTAT 10.2 (Systat Software Inc., San Jose, CA) to detect significant differences in water absorption according to the different predictors (*dolium*, lithobiontic community, season).

## 3. Results

### 3.1. Microclimatic monitoring of *dolia* and sculptures' locations

Even though data of T and RH of the garden and the terrace referred to a short period (July 2021–June 2022), nonetheless they provided relevant indications about the climatic conditions of the two places. Although the two locations of the *dolia* and the sculptures are housed in the same building, the environments are quite different. The garden is a meadow at ground level with some trees and surrounded by the museum buildings. The terrace, on the second floor, is totally exposed to sunlight, is made of a light stone and is close to the adjacent roof made of metal. These materials contribute to creating a peculiar microclimate in summer with high temperature and low RH.

In July and August 2021, the average values of T and RH were  $26.1^\circ\text{C}$  and  $57.8\%$  in the garden, and  $28.2^\circ\text{C}$  and  $50.7\%$  RH in the terrace. These values appear rather similar but, observing the single series of data, it appears that in many days the temperature in the terrace reached values around  $52^\circ\text{C}$  (Fig. S1), while the maximum temperatures in the garden were not higher than  $40^\circ\text{C}$ . These latter values are similar to the maximum temperatures of the city of Faenza registered by the Osservatorio Meteorologico Torricelli (Table S2). The data of February–June 2022 confirmed the trend (Fig. S1). In March, the terrace's temperature reached  $32^\circ\text{C}$  on some days, and in April, May and June there were values around  $30\text{--}35^\circ\text{C}$ ,  $40^\circ\text{C}$  and  $45\text{--}50^\circ\text{C}$ , respectively. The RH had many oscillations and variations (around  $20\text{--}85\%$  in March, April and May, around  $20\text{--}54\%$  in June). In the garden, T and RH were instead close to the values registered by the Osservatorio Meteorologico Torricelli. Therefore, the temperature and RH values lead to define the terrace microclimate as fairly extreme in summer. The climatic variation between the two places changed in the second half of September 2021 even though the differences remained, with higher T and lower RH in the terrace than in the garden (October average values  $15.0^\circ\text{C}$  and  $77.6\%$  RH in the terrace,  $13.6^\circ\text{C}$  and  $82.8\%$  RH in the garden). In winter (2021/22) the av. value of temperature was  $4.6^\circ\text{C}$ , similar to that of the dataset 2011–2021, while the RH av. value  $91.7\%$  was quite far from RH  $75\%$  of the dataset.

### 3.2. Archaeometric characterization of *dolia* and sculptures

The big *dolium* inv. 10366,1 showed a very coarse body characterized by inclusions (maximum size about 2 mm, around  $10\%$  in volume) of volcanic origin (pumice, basalt fragments with needle-like microcrystals of plagioclase, phenocrystals of plagioclase and pyroxenes, olivine, and rare hornblende), and by iron nodules (Fig. S2). The natural aplastic inclusions ( $<100 \mu\text{m}$ ) had the same origin as the coarse grains.

The microstructure of the small *dolia* was different from that of inv. 10366,1 as the matrix was very fine and homogeneous (Fig. S3). The abundance of natural aplastic inclusions was around  $15\%$  in volume. The minero-petrographic composition mainly consisted of a clayey raw material with silicate detrital grains such as quartz, feldspars, and micas. Iron nodules were also present.

Regarding the chemical compositions (Table 1), the sample from inv. 10366,1 showed the lowest calcium content ( $\sim 4\%$  CaO) and the highest iron content ( $\sim 11\%$   $\text{Fe}_2\text{O}_3$ ), the latter connected to the iron nodules and the volcanic grains identified in thin section. The four small *dolia* contained medium calcium content (CaO  $> 5\%$ ). The sample from inv. 19074 had a quantity of  $\text{SO}_3 > 2\%$ , due to degradation phenomena.

**Table 1**

Anhydrous chemical composition (% by weight of oxides), open porosity (%) and prevalent pore size ( $\mu\text{m}$ ) of *dolia* and sculptures.

	INV. 10366,1	INV. 19074	INV. 19075	INV. 19076	INV. 19077	Mazzini	Tsivin
SiO <sub>2</sub>	56.88	58.62	55.15	57.33	58.72	n.a.	n.a.
Al <sub>2</sub> O <sub>3</sub>	20.06	15.43	16.66	17.84	19.07	n.a.	n.a.
TiO <sub>2</sub>	1.46	1.07	0.98	1.09	0.97	n.a.	n.a.
Fe <sub>2</sub> O <sub>3</sub>	11.07	7.86	8.89	8.02	7.43	n.a.	n.a.
CaO	4.33	8.32	12.77	9.00	7.31	n.a.	n.a.
K <sub>2</sub> O	2.54	3.16	2.77	3.61	2.70	n.a.	n.a.
Na <sub>2</sub> O	1.03	0.91	0.81	0.87	1.34	n.a.	n.a.
MgO	2.25	1.71	1.85	2.03	2.19	n.a.	n.a.
P <sub>2</sub> O <sub>5</sub>	0.38	0.18	0.12	0.22	0.26	n.a.	n.a.
SO <sub>3</sub>	0.00	2.73	0.00	0.00	0.00	n.a.	n.a.
Pore size	0.2–10	0.4–0.7	0.4–0.7	0.4–0.7	0.4–0.7	0.03–5	0.3
Porosity	28.65	41,22	36.03	37.41	36.01	28	27

The mineralogical composition, quite similar in the five *dolia*, was characterized by quartz, anorthite, pyroxene, gehlenite, illite/mica and traces of hematite. Calcite peaks were also detected in all samples but inv. 19075. Gypsum and hexahedrite were detected in *dolia* 19074 and 19075, respectively. The presence of gypsum confirmed the deterioration by external pollution, as suggested by the chemical composition.

Information about the highest firing temperatures depends on the presence or absence of primary calcite, hematite, illite, diopside and gehlenite. The neoformation phases and the contemporary presence of illite allowed to hypothesize a maximum temperature of 900 °C (Gliozzo, 2020). A higher firing temperature is estimated for inv. 19075 because of the absence of illite/mica (Ricciardi et al., 2007).

The two sculptures displayed different microstructures. The sample from Tsivin's sculpture showed a ceramic matrix with well distributed aplastic inclusions (<100  $\mu\text{m}$  in size and around 10 % in volume) made of silicate grains such as quartz and feldspars. The coarse inclusions (dimensions greater than 500 $\mu\text{m}$  and approx. 3 % in volume) consisted of quartz grains, residues of chamotte and crystals of moissanite (SiC - silicon carbide) (Fig. S4). Interestingly, the Py-GC-MS analysis, carried out without the silylating agent, identified the characteristic pyrolytic profile of casein (pyrrole, toluene, methylphenol, benzeneacetonitrile, benzenepropanonitrile and dichetopiperazine - DKPs) (Orsini et al., 2017). The analysis also identified a quite high amount of levoglucosan, derived from the pyrolysis of a polysaccharide, and aliphatic hydrocarbons attributable to a paraffin. The same analysis carried out with the silylating agent (Fabbri and Chiavari, 2001) confirmed the presence of the polysaccharide and identified a lipid characterized by a fatty acid profile with a relatively high abundance of lactic and myristic acids (data not shown). The copresence of this lipid with polysaccharide and casein suggests the use of milk or powdered milk added to the ceramic by the artist.

The sample from Mazzini's sculpture showed a brownish ceramic matrix (Fig. S5) composed of quartz and feldspars (grains in the range 100–250 $\mu\text{m}$  and 10–15 % in volume). The coarse inclusions (up to 1 mm) were grogs of highly fired ceramics and metamorphic rock fragments (probably micaschists) with evident alteration patterns. A very thin dark layer was present on the external surface (Fig. S5).

The mineralogical composition of both sculptures was indicative of a typical stoneware ceramic paste probably obtained by using kaolin as main clayey raw material. Tsivin's artwork contained mullite, corundum, cristobalite, quartz and moissanite, while Mazzini's sculpture only cristobalite and mullite. Moissanite is an artificial product that was intentionally added by the artist and probably used as a temper with aesthetic purpose, i.e., to give a high brilliance to the paste.

### 3.3. Porosimetry measurements of *dolia* and sculptures

The total open porosity measurements confirmed the differences between the big *dolium* (inv. 10366,1) and the small four. The pore size distribution graph of inv. 10366,1 shows a Gaussian's curve in which the mode,

the most frequently occurring size-class, coincides with the pores with a diameter around 0.2  $\mu\text{m}$  (Fig. 2a). However, the graph shows a bimodal pore size distribution with a less frequent mode of pores around 10  $\mu\text{m}$ . The shape of the curve is likely the result of degradation that affected the microstructure causing the decreasing of small pores and the consequent increase of percentage number of big pores, or the partial or total closing of big pores leading to the main presence of small pores. However, the second hypothesis is unlikely as the percentage of the cumulative pore volume is very high in correspondence to the small pores. The total open porosity is 28.65 %.

The pore size distribution curves of the four small *dolia* are quite similar (Fig. 2b). They are Gaussian's curves with a small tail towards pores with smaller diameters that could be due to substrate alteration. The mode and median are almost coincident and the most frequently occurring size-class is in the range 0.4–0.7  $\mu\text{m}$ . The total open porosity is around 36–41 %, higher than the big *dolium*. This type of curve suggests a good level of treatment of the clayey raw materials, that caused a high level of sorting and so a substantial homogeneity of dimensions.

As regards the sculptures, the porosimetry curves indicate specific microstructures. The ceramic body of Mazzini's sculpture is characterized by a bi-modal pore distribution (Fig. S6). The first mode is in the micropores area and coincides with the 0.03  $\mu\text{m}$  diameter dimensional class, while the second mode, the most frequently occurring, corresponds to the 5  $\mu\text{m}$  size-class. The spatial range of pore diameter is comprised between 0.008 and 100  $\mu\text{m}$ . The total open porosity is 28 %.

On the contrary, the pore distribution curve of Tsivin's artwork is a Gaussian's curve with a right asymmetric tail in the macropore area (Fig. S6). The class of pores with diameter 0.3  $\mu\text{m}$  is the modal class and the median is shifted towards the right side and coincides with the 0.7  $\mu\text{m}$  size-class. The total open porosity is around 27 %. The spatial range of pore diameter is between 0.008–100 $\mu\text{m}$ .

Polarized light optical microscopy of thin sections of the two sculptures showed pores (>100 $\mu\text{m}$ ) with different shapes. As for Mazzini's sculpture, the porosity was low and mainly formed by voids that surrounded the large inclusions and were caused by clay matrix shrinkage. Some ring-shaped voids were due to the kneading process.

### 3.4. The biological colonization of the *dolia* and the sculptures

The biological colonization of the *dolia* and the sculptures is morphologically characterized as layers of variable thickness, extension, and color, mainly due to the development of epilithic crustose lichens and biofilms.

The colonization was similarly distributed on the surfaces of the small four *dolia*. The areas above the major curvature were quite entirely covered by lichens, particularly the edges of the openings (excluding the parts protected by metal covers) and the surfaces immediately below (Fig. 3). Areas below the major curvature and next to the ground were predominantly colonized by green-algal biofilms or uncolonized. Thus, the average biological cover percentages of these *dolia* ranged from 66 to 86 %. Diversely, the big *dolium* was characterized by a different and unevenly distributed colonization in comparison to the others (Table 2 and vide infra), with lichens and mosses mostly limited to the upper north-facing area. The surface facing south-west and the bottom part (around 60 cm from the ground) were almost completely lacking colonization. The average lithobiontic cover percentage was about 20 %.

Twenty-two lichen species were listed (Table 2), which, with reference to ecological indicator values (Nimis, 2022), mostly share tolerance of high (direct) solar irradiation (max SI 4–5), xeric conditions (max AR 4–5), rather eutrophicated situations (max EU 4–5), and are reported for highly disturbed synanthropic areas (max PO 3). The presence of few hygrophytic species (max AR 2) was only remarkable on the north-facing and bottom parts of some *dolia*.

On the small *dolia*, the quite continuous lichen mosaic above the major curvature (inclination between 30° and 65°) was dominated by the crustose species *Lecanora campestris*, *Lecidea fuscoatra*, *Protoparmeliopsis muralis* and *Verrucaria nigrescens* (Table S3). The foliose lichens *Phaeophyscia orbicularis* and *Physcia adscendens* also occurred in limited areas. Along the major

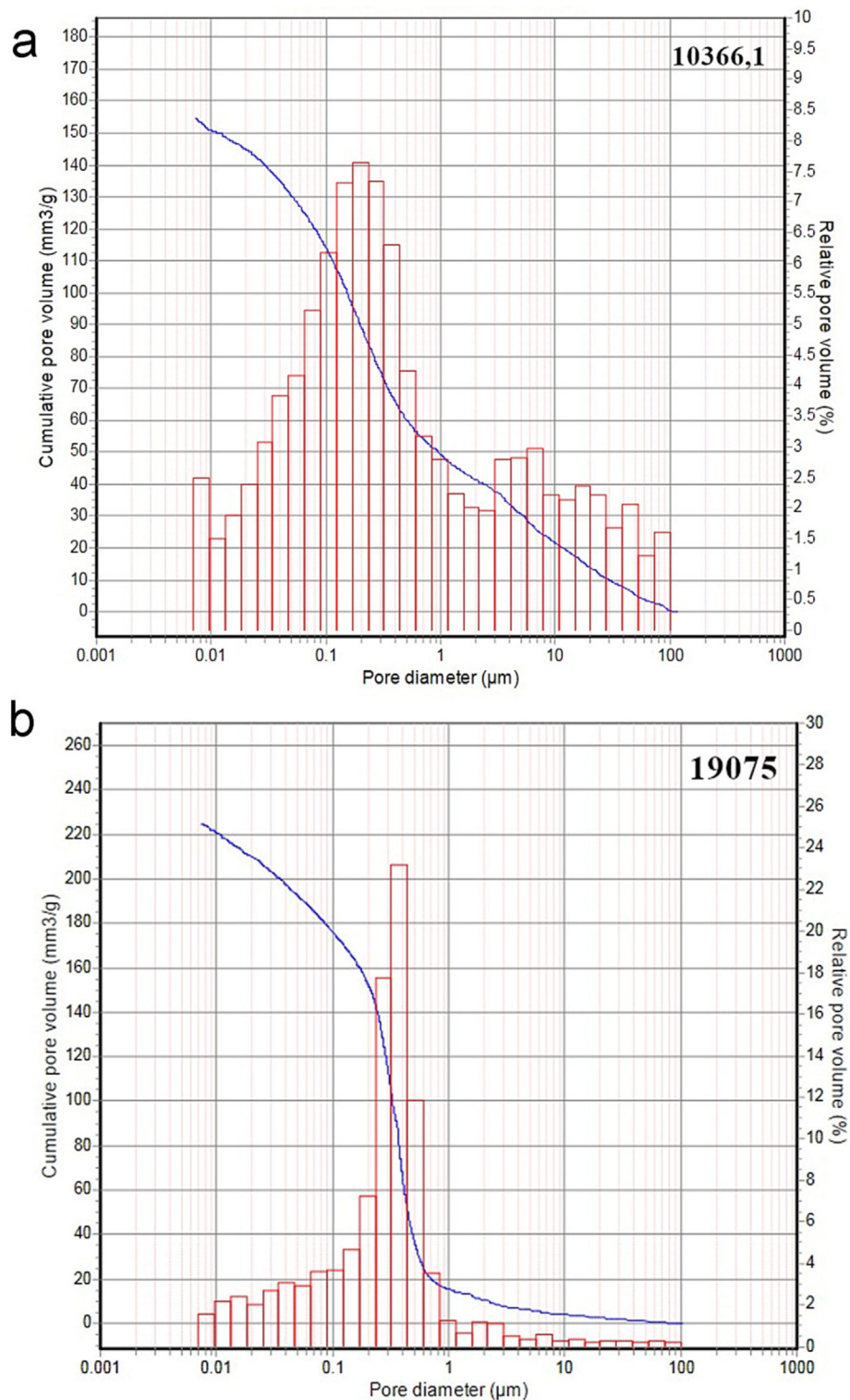


**Fig. 2.** Open porosity (cumulative pore volume, blue line) and pore size (relative pore volume, red histograms) of (a) inv. 10366,1 - the big *dolium*, and (b) inv. 19075 representative of the four small *dolia*.

curvature (inclination around 90°), the copious growth of *Flavoplaca citrina* was present. A black-gray layer widely covered parts of the *dolia*, mainly on the major curvature and below it. At first observation, it was seemingly formed by lichens and biofilms. The layer was very thin, just some hundred microns, and its distribution on the surface was uneven. The observations with the hand lens and the microscopic analysis of layer's fragments demonstrated that it was a sort of mosaic formed by the lichens *Verrucaria nigrescens* and *Acarospora gallica* and by primordia of other crustose unidentifiable

species. In this mosaic, few thalline areoles were healthy while the others were visibly overgrown by a biofilm dominated by black meristematic fungi (Fig. 4a) that, at various degrees, caused eventually the disappearing of the lichens. This black-gray layer (characterization by metabarcoding in Section 3.5) occupied a more extensive surface on the *dolia* inv. 19074 and 19076, where it also dominated above the major curvature.

As for the big *dolium*, the number of lichen species was lower than that of small *dolia*. On the part facing north below the opening's edge, a large

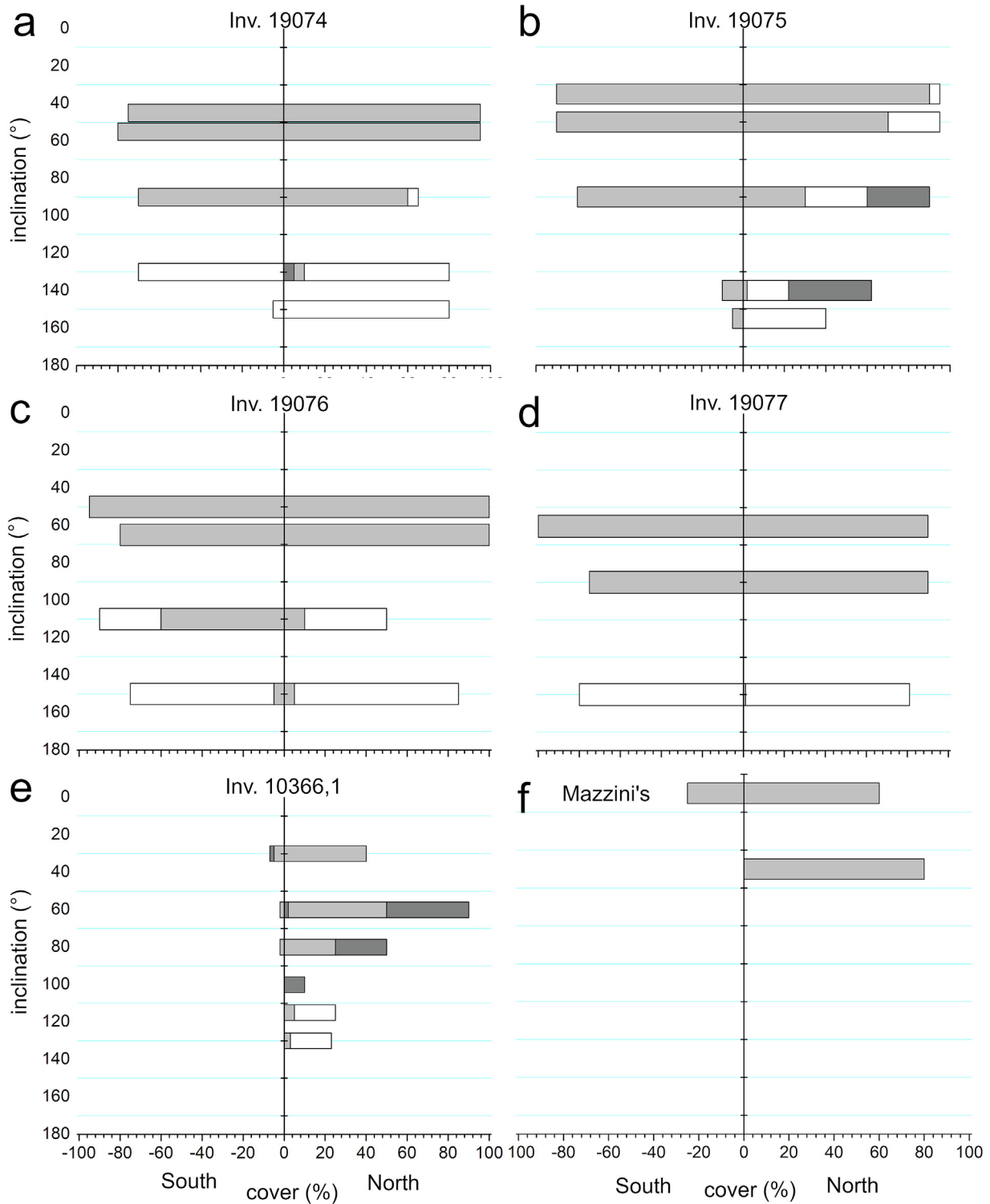


**Fig. 3.** Distribution of biological coverage (%) on terracotta by lichens (light gray bar), algal biofilms (white bar), and mosses (dark gray bar) as a function of the inclination of surfaces of the *dolia* and Mazzini's sculpture.

lacuna composed of cement, a material different from the original terracotta, hosted sparse thalli of *Myriolecia dispersa* and *M. albescens*. The lichen *Lecidea fuscoatra* and mosses were also found in this area and in the close terracotta, while the hygrophytic *Scoliosporum sarothamni* was abundant on terracotta parts close to the ground. On the part facing south, lichen colonization was extremely poor (max cover above major curvature 5%) and mostly due to *Verrucaria nigrescens*. The part facing north-east had a

more widespread colonization, mainly formed by green and black biofilms, and the lichens *Flavoplaca citrina* and *Lecidea fuscoatra*. The green and black biofilms were mainly composed by coccoid (*Trebouxia* sp.) and filamentous (*Ulothrix* sp.) green algae, and were well developed only in this area where, presumably, there were a micro-niche peculiar for its environmental conditions, and very favorable to the algae. Although the biofilm was seemingly formed only by algae, the observation of cross sections displayed a different



**Table 2**

The biological colonization of *dolia* and sculptures. For each lichen species, ecological indicator values (Nimis, 2022) are reported: pH of the substratum (pH), solar irradiation (SI), aridity (AR), eutrophication (EU) and poleotolerance (PO) [ordinal scales for each index available at <https://italic.units.it/index.php?procedure=base&t=59&c=60>].

Biological colonization	pH	SI	AR	EU	PO	Inv. 10366,1	Inv. 19074	Inv. 19075	Inv. 19076	Inv. 19077	Volumes by Tsvin	Big machine that grinds by Mazzini
Lichens (tot. species)						x (9)	x (14)	x (15)	x (16)	x (8)	x (1)	x (7)
<i>Acarospora gallica</i> H. Magn.	2–3	3–5	4	3–4	1–2	x	x	x	x	x	x	x
<i>Brianaria sylvicola</i> (Körb.) S. Ekman & M. Svenss.	1–2	1–2	2	1	1	x	x	x	x	x		
<i>Candelaria concolor</i> (Dicks.) Stein	3–4	4–5	3–4	3–5	1–3			x				
<i>Candelariella vitellina</i> (Hoffm.) Müll. Arg.	1–3	3–5	3–4	2–5	1–3			x	x			x
<i>Circinaria hoffmanniana</i> (S. Ekman & Fröberg ex R.Sant.) A. Nordin	3–5	3–5	3–4	3–5	1–3		x		x	x		
<i>Flavoplaca</i> gr. <i>citrina</i> (Hoffm.) Arup, Frödén & Søchting	3–5	4–5	3–4	4–5	1–3	x	x	x	x	x		
<i>Gyalolechia flavovirescens</i> (Wulfen) Søchting, Frödén & Arup	3–4	3–4	3	3–4	1–2							x
<i>Lecania turicensis</i> (Hepp) Müll. Arg.	3–5	3–4	3	4–5	1–3			x		x		
<i>Lecanora campestris</i> (Schaer.) Hue	2–4	4–5	3	2–3	1–3		x	x	x			
<i>Lecidea fuscoatra</i> (L.) Ach. (including <i>Lecidea grisella</i> Flörke)	2–3	4–5	3–5	2–4	1–3	x	x	x	x			
<i>Myriolecis albescens</i> (Hoffm.) Šliwa, Zhao Xin & Lumbsch	3–5	3–5	3–5	3–4	1–3	x	x	x	x			x
<i>Myriolecis dispersa</i> (Pers.) Šliwa, Zhao Xin & Lumbsch	4–5	3–5	4–5	2–4	2–3	x	x	x	x	x		x
<i>Phaeophyscia orbicularis</i> (Neck.) Moberg	2–5	3–5	3–4	4–5	1–3		x	x	x			
<i>Physcia adscendens</i> H. Olivier	2–5	4–5	3–4	3–5	1–3			x	x			
<i>Protomeliopsis muralis</i> (Schreb.) M. Choisy	2–4	3–5	3–4	3–5	1–3		x	x	x			x
<i>Scoliosporum sarothamni</i> (Vain.) Vězda	2–3	2–3	2	1–2	1	x	x	x	x			
<i>Verrucaria nigrescens</i> Pers. f. <i>nigrescens</i>	3–5	3–5	2–5	2–5	1–3	x	x	x	x	x		x
<i>Xalocoa ocellata</i> (Fr.) Kraichak, Lücking & Lumbsch	4–5	4–5	3–4	2–3	1–2				x			
<i>Xanthocarpia crenulata</i> (Nyl.) Frödén, Arup & Søchting	4–5	4	3–4	4	1–2		x		x			
<i>Xanthoparmelia</i> sp. (young brown thallus)						x						
<i>Xanthoria parietina</i> (L.) Th. Fr.	2–4	3–5	3–4	3–4	1–3			x				
Unidentified sorediate crustose taxon (R-)										x		
Mosses						x	x	x				
Algal biofilms						x						
Prominent growth of black fungi on and beneath lichens							x	x	x	x		x
Black fungi											x	

“scene” because just below the surface there were colonies of black meristematic fungi arranged in clumps (Fig. 4 m, n, o). The algae, instead, grew on the surface and did not diffuse in the substrate.

Lichen colonization on Tsvin's artwork was extremely scarce (Fig. 1b), limited to few sparse thalli of *Acarospora gallica* on the legs' surfaces. Differently, lichen cover was remarkable on the horizontal surface of Mazzini's statue (Fig. 1c), including most of the species already reported for the *dolia* (Table 2), and the black-gray layer also occurred.

### 3.5. Metabarcoding of the lichen-associated microbial communities

High quality ITS2 sequences obtained from the black-gray layer ranged between 25,219 (inv. 19074) and approx. 13,000 (inv. 10366,1 and Mazzini's sculpture). A single OTU was recognized from sparse black mycelia on Tsvin's sculpture. Ninety fungal OTUs were inferred, of which 18 % were shared by more than one investigated surface (Fig. 5a). Most OTUs were attributable to Ascomycota (av. 59 %), a few to Basidiomycota, Chytridiomycota and Mortierellomycota (5 %), while others were taxonomically unidentifiable (36 %; Table S4a).

In samples from the big *dolium* and Mazzini's sculpture, readings attributable to lichen-forming fungi of genera *Verrucaria* (Verrucariales, Eurotiomycetes) and *Acarospora* (Acarosporales, Lecanoromycetes) strongly prevailed (approx. 90 %), while they subordinately occurred in the case of the smaller *dolium* inv. 19074 (36 %) (Fig. 5c). On this latter, readings attributable to non-lichenized fungi of genus *Knufia* (Chaetothyriales, Eurotiomycetes) were prevalent. Other non-lichenized fungi of classes Dothideomycetes (with OTUs mostly attributable to genera *Devriesia* and *Extremus*, Capnodiales, and to *Didymella* and *Alternaria*, Pleosporales), Eurotiomycetes (with OTUs attributable to genera *Cladophialophora*, *Coniosporium* and *Exophiala*, Chaetothyriales) and Sordariomycetes (with OTUs mostly attributable to genus *Fusarium*) abundantly occurred in terms of OTUs and readings on the *dolia* and on Mazzini's sculpture. The single OTU from Tsvin's sculpture was attributed to *Cladosporium* sp.

High quality 16S sequences, achieved from the same scraped layers, ranged between 4000 and 1300 and were assigned to a total of 120 OTUs, of which 15 % were shared by more than one surface (Fig. 5b; Table S4b). Readings ascribable to chloroplastic DNA of green algae

abundantly occurred (19 % of the total) (Fig. 5d). Other OTUs are mostly segregated in phyla Proteobacteria (mostly Alphaproteobacteria), Actinobacteria, and Bacteroidetes (mostly Cytophagia), with the number of unidentified sequences being only remarkable in the case of the sample from Mazzini's sculpture.

### 3.6. The interaction of lichens and the black-gray layer with the terracotta

Microscopical observations of cross sections showed species-specific patterns of penetration within the terracotta. *Protomeliopsis muralis* did not deeply diffuse in the substrate even though the thallus was well developed and spread on the surfaces. Observing the cross sections stained with PAS, it appeared that the hyphal penetration component propagated inside the substrate only locally and down to approx. 200  $\mu$ m (Fig. 4 g, h, i). However, quartz and feldspar crystals on the surface have been detached by the hyphal expansion. Similarly, *Lecanora campestris* did not deeply penetrate within the substrate (up to 500  $\mu$ m), but a dense network of hyphae pervasively developed down to 400  $\mu$ m and was able to envelop and detach terracotta fragments (Fig. 4j).

PAS-stained cross sections of *Lecidea fuscoatra* showed hyphae inside the substrate down to around 1 mm, but the majority were located in a sublayer of about 300  $\mu$ m from the surface where they wrapped terracotta particles such as big quartz crystals and fragments containing iron that were present inside the thallus (Fig. 4 k, l). The hyphal penetration component of this lichen was less abundant than that of *Lecanora campestris*.

Although the thallus of *Verrucaria nigrescens* was thin, it included fragments of the substrate in its carbonaceous basal layer. Its hyphae have been found in high amounts inside the substrate at >1 mm from the surface (Fig. 4 e, f).

The terracotta under the black-gray layer was colonized by a dense network of hyphae belonging either to the lichen mycobionts or to the lichen-associated fungi (Fig. 4 b, c, d). The hyphae diffused a lot into the substrate, going into voids, surrounding iron minerals and quartz and feldspar crystals down to around 2 mm, and forming clusters of hyphae inside (Fig. 4 b, c, d). It appeared to be a very peculiar pattern of colonization, in which the biological development began with lichens (mainly *Verrucaria nigrescens* and

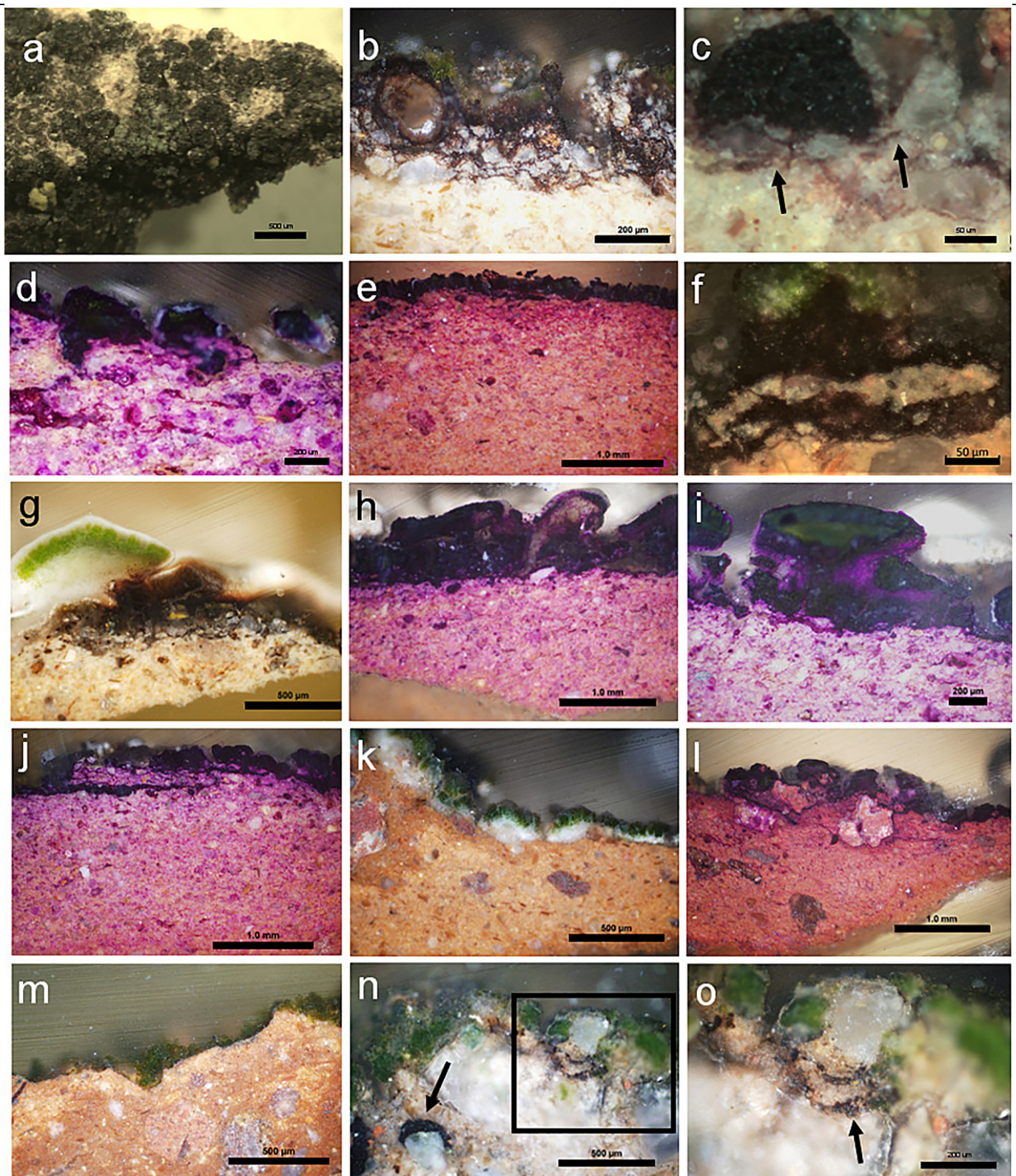


**Fig. 4.** Lithobiontic colonization of the *dolia*. a) Stereoscopic image that shows the black-gray layer formed by lichens overgrown by a biofilm of black fungi; b) cross sections of *Verrucaria nigrescens* showing its carbonaceous black-basal layer that diffuses into the substrate, surrounds crystals, forms clusters and affects the lichens' structure; c) cross section showing meristematic black fungi (arrows) penetrating beneath the lichen thalli; d) the microphotograph shows the section of lichens parasitized by fungi stained with PAS that makes well visible the compact network of hyphae, belonging either to the lichens or to the fungi, that grows into the substrate; e, f) cross sections (one stained with PAS) of the lichen *Verrucaria nigrescens* showing fragments of the substrates incorporated in the thallus and the hyphal diffusion into the substrate; g, h, i) cross sections before and after staining with PAS of the lichen *Protoparmeliopsis muralis*; j) cross sections stained with PAS of the lichen *Lecanora campestris* showing terracotta fragments surrounded by thallus and penetrating hyphae; k, l) cross sections of the lichen *Lecidea fuscoatra* before and after staining with PAS; m, n, o) inset of n) cross sections of algal biofilms and black meristematic fungi on *dolium* inv. 10366,1 displaying the hyphal diffusion within the substrate (arrows). Scale bars: 50  $\mu\text{m}$  (f), 200  $\mu\text{m}$  (b, c, d, i, o), 500  $\mu\text{m}$  (g, k, m, n), 1 mm (e, h, j, l).

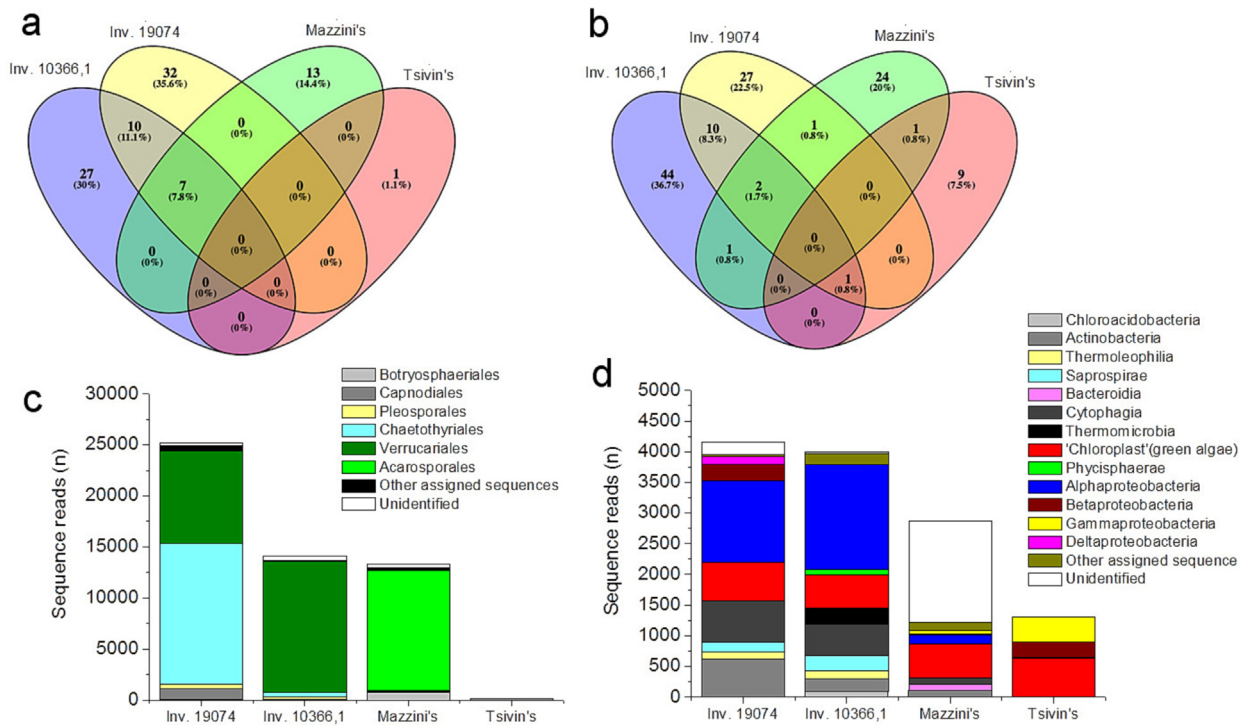


Fig. 5. Metabarcoding results. Venn diagrams showing the number of shared fungal (a) and bacterial (b) OTUs between samples from inv. 10366,1, inv. 19074, and Tsivin's and Mazzini's sculptures; number of sequence reads for (c) the different orders of fungi and the different classes of bacteria (d) on the big *dolium* (inv. 10366,1), a representative small *dolium* (inv. 19074), and on Mazzini's and Tsivin's sculptures.

*Acarospora gallica*) and then black fungi overgrew the lichens and eventually prevailed on them.

3.7. Water absorption and substrate hardness of surfaces uncolonized and colonized by lichens and biofilms

GLM analyses showed a significant contribution of both the measuring time (F-ratio = 6.245, P = 0.003) and the presence/type of lithobiotic cover (F-ratio = 3.163; P = 0.048) in regulating the substrate water absorption (W<sub>a</sub>) measured by contact sponge method (Table 3a). Table 3b

reports the W<sub>a</sub> values of the three considered *dolia* - the big one and inv. 19074 and 19075 - as representative of the total biological colonization. In December 2020 the values were low because the substrate retained air humidity and rainwater, while in May and October 2021 it was drier. However, regardless of the climate, it is worth noting that the W<sub>a</sub> values of the uncolonized spots are always, but in one case, higher than that of colonized areas. The values of water absorption over time of spots characterized by the continuous covering of lichens on *dolia* inv. 19074 and inv. 19075 (mostly *Protoparmeliopsis muralis* and *Lecanora campestris*) were lower than those of uncolonized spots (Table 3b). The same behavior was

Table 3

Water absorption (W<sub>a</sub>). (a) Summary of the generalized linear model on measurements performed before the lithobiotic removal. (b) W<sub>a</sub> measurements (mg cm<sup>-2</sup> min<sup>-1</sup>) collected in different seasons on surfaces colonized by lichens and biofilms, and uncolonized (average values ± SD). At each measuring time and, separately, for the big and the small *dolia*, measurements not sharing at least one letter are significantly different (ANOVA with Tukey's *post-hoc* test; P < 0.05). (c) Measurements on small *dolia* after the removal of lithobiotics. Measurements not sharing at least one capital letter are significantly different (ANOVA with Tukey's *post-hoc* test; P < 0.05); asterisks indicate significant differences with respect to measurements collected in the same season, but before the removal of lithobiotics.

a	Parameter	Source	Sum of squares	df	Mean-Square	F-ratio	P			
	Absorbed water	Dolia	0.157	2	0.079	2.336	0.104			
		Lithobiotics	0.213	2	0.106	3.163	0.048			
		Season	0.420	2	0.210	6.245	0.003			
		Error	2.525	75	0.034					
b	Season <i>Dolia</i>	Inv. 10366,1	W <sub>a</sub> (mg cm <sup>-2</sup> min <sup>-1</sup> )	Inv. 19074 & 19075	Lithobiotics	W <sub>a</sub> (mg cm <sup>-2</sup> min <sup>-1</sup> )				
		Winter (2020.12.14)					Lichens [mostly <i>L. gr. fuscoatra</i> ]	0.25 ± 0.05 (a)	Lichens [mostly <i>P. muralis</i> , <i>L. campestris</i> ]	0.24 ± 0.13 (a)
		Spring (2021.05.18)						0.67 ± 0.05 (a')		0.84 ± 0.64 (a')
		Autumn (2021.10.05)						0.69 ± 0.26 (a'')		1.49 ± 1.25 (a'')
		Winter (2020.12.14)					Biofilm [green black biofilm of algae and fungi]	0.67 ± 0.41 (a)	Biofilm [black-gray layer of fungi overgrowing <i>V. nigrescens</i> ]	0.38 ± 0.24 (a)
		Spring (2021.05.18)						1.17 ± 0.10 (b)		0.98 ± 0.47 (a')
		Autumn (2021.10.05)						2.52 ± 0.87 (b'')		2.04 ± 0.64 (ab'')
		Winter (2020.12.14)					Uncolonized	0.50 ± 0.12 (a)	Uncolonized	1.10 ± 0.38 (b)
		Spring (2021.05.18)						0.75 ± 0.13 (a')		2.38 ± 1.09 (b')
		Autumn (2021.10.05)						0.8 ± 0.42 (a'')		3.55 ± 1.43 (b'')
c	Winter (2022.12.16)	Lichens (after removal)				0.72 ± 0.32 (A)*				
		Biofilm (after removal)				2.13 ± 0.86 (B)*				
		Uncolonized				1.68 ± 0.81 (AB)				

accomplished by areas with the black-gray layer of fungi overgrowing *Verrucaria nigrescens*, which took a bit more water than the lichen mosaics. The above-mentioned exception regarded the areas with thin green-black algal biofilm of inv. 10366,1 that absorbed an amount of water much higher than that of uncolonized spots. This was more noticeable in the measures of May and October 2021, when there were low water quantities in the substrate. In October 2021 the spot with the green-black algal layer and the uncolonized one displayed values of  $W_a$  equal to 2.52 and 0.80, respectively. Nevertheless, on a statistical basis, the influence of physical characteristics, such as porosity, of this *dolium* was not significant (F-ratio = 2.336,  $P > 0.05$ ).

On a new winter season, after the removal of the lithobionts (Table 3c), the surfaces of *dolia* inv. 19074 and inv. 19075 previously covered by the continuous lichen mosaic of *P. muralis* and *L. campestris*, and by the black-gray layer of fungi associated to *V. nigrescens*, showed  $W_a$  values higher than the previous ones. However, the surfaces earlier covered by the continuous lichen mosaic still displayed lower values than those of the uncolonized surfaces. By contrast, those previously colonized by the black-gray layer showed the highest  $W_a$  values.

Sclerometric measurements by Equotip showed average values of surface hardness ranging between 415 and 450 Leeb units (Fig. 6). Remarkably, surface hardness values measured beneath the thalli of *Verrucaria nigrescens* were significantly lower than those of surfaces colonized by *Protopermeliospora muralis* and of uncolonized surfaces. These micro-areas displayed similar hardness.

#### 4. Discussion

Porosity has been indicated as a crucial factor driving the bioreceptivity of ceramic materials, because of its influence on the absorption and movement of water, and thus on the water availability for microorganisms (Coutinho et al., 2015). In this work, different ceramic objects exhibited different porosity values that relate to i) production processes, ii) chemical and mineralogical composition of the raw materials, iii) the firing conditions and iv) environmental and microbial weathering (Tschegg, 2009) (see Sections 3.3 and 4.1). According to the previous literature, ceramics displaying higher porosity showed higher bioreceptivity, although environmental differences caused by objects' different geometries and/or locations may also contribute to the observed colonization patterns. On the other hand, this study supported the proposed hypothesis that lithobiotic colonization influences physical properties related to artworks' durability, combining negative effects for conservation as the detachment of mineral fragments and a species-specific surface hardness reduction,

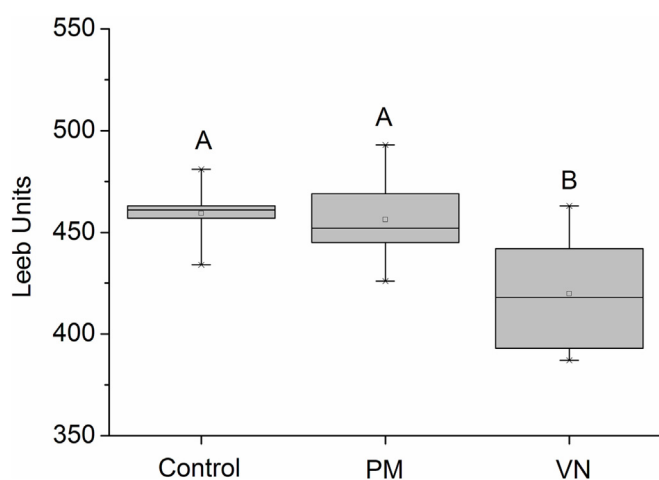


Fig. 6. Surface hardness (Single Impact Measurement) of *dolia* in areas colonized by *Protopermeliospora muralis* (PM) and *Verrucaria nigrescens* (VN), and uncolonized (Control). Boxplots not sharing at least one letter are significantly different (ANOVA, Tukey's test;  $P < 0.05$ ).

with positive ones as the reduction of water absorption, at least until the lithobionts are not removed from the ceramic surface.

The provenance of the *dolia*, the relationships between archaeometric production processes and substrate porosity, the influence of this latter on lithobiotic colonization in combination with other microenvironmental factors, and the impact of different lithobiotic components - including lichens, algal biofilms, and associated fungi - on the substrate physical properties are detailed in the next sub-sections.

#### 4.1. Archaeometric results

The results of the archaeometric investigations provided notable information about *dolia*'s provenance. After comparing the composition and microstructure of the small *dolia* with some Roman ceramics found in the Apulian territory (Glozzo et al., 2019), a good compatibility appeared. So, according to Glozzo et al. (2018), it was plausible to hypothesize the use of materials of the clay deposits in the area close to Gargano and in the Ofanto valley, which are sub-Apennine marly-silty clays with surface sandy lenses.

Following the museum's documentations, the big *dolium* was instead compared with ceramics and lithic artifacts from Sicily, in particular from the Etnean area. Franco and Capelli (2014) identified a group of wine amphorae of the period from 1st to 6th century BC characterized by elements of volcanic origin (fragments of basalts, derived plagioclase, and pyroxene from lava effusions of Etna), and by a quartzitic and sedimentary component, as production of the Etna/Catania area. The ceramic paste of the big *dolium* fitted well with the above-reported description. Its provenance from the Etna area was also supported by comparison with millstones crafted with volcanic stones outcropping in the Messina territory (Di Bella et al., 2016).

Considerations regarding the physical properties of ceramics and, thus, of the artworks under examination are worth mentioning. The microstructure, including porosity, and the firing temperature are key factors that affect the state of conservation of ceramics (Coletti et al., 2016; Maritan, 2020). In particular, porosity and pore size distribution deeply influence the durability of the ceramic materials more than other physical or mechanical properties. It is worth noticing that the pore structure is formed during the ceramics production and is influenced by the chemical and mineralogical composition of the raw materials, and by the firing conditions. Open porosity connects the interior parts of ceramics with the external environment causing the potential fluids' storage and their circulation. The effective porosity, which includes the open and the interconnected pores, can favour the circulation of the fluids and then constitutes the main pathway for the damage (Anovitz and Cole, 2015). According to the literature (Cultrone et al., 2004; Jordan et al., 2008), a considerable decrease in the porosity and a beginning of vitrification occurs at firing temperatures between 1050 and 1100 °C, with a consequent decrease of the pore radius. The increase of the firing temperature causes a progressive elimination of the smaller pores due to the increase of the liquid phase (Amoros et al., 1992). The results can vary when coarse inclusions are present in the ceramic paste. It could be the case of the big *dolium* and the two sculptures where the coarse inclusions can contribute to the formation of pores and voids. The two clusters of pores of these artworks not only influence the water absorption but also the rate of water diffusion. In contrast, the microstructure of the small *dolia* is very fine. Most of the pores are characterized by diameters ranging 0.01–1.00 μm, which likely do not favour the diffusion of percolation solutions inside the ceramic paste.

#### 4.2. Ceramic bioreceptivity to lichen and biofilm colonization

The detection of lichens and microbial communities on the examined objects reflects the well-known high bioreceptivity of stone substrates located outdoors, and in particular of ceramics (Coutinho et al., 2015). Most lichen species colonizing the *dolia* and the sculptures are common constituents of lichen communities on siliceous stone heritage surfaces, which often share xerophytism and photophytism -related to direct sun irradiation- and nitrophytism -related to the location in green areas (Nimis et al., 1992). With this regard, the location of the *dolia* in the center

of the MIC garden on a meadow perfectly displays the mentioned environmental conditions, while that of the sculptures on the building terrace only agrees with the highly irradiated and xeric conditions, while not with a high nutrient availability, a fact that likely partially explains the lower colonization observed on Mazzini's and Tsvini's works. On the other hand, geometric features and the quantified differences in porosity of the *dolia* and the two sculptures may further contribute to explain different lichen covers as well as the different diffusion of microbial biofilms. In particular, the big dimension of *dolium* inv. 10366,1 together with its (sub-)horizontal surfaces above the major curvature at about 140 cm from the ground and the low porosity values, are likely less favorable to organic (dust) deposition and water availability. Accordingly, lichen colonization on this *dolium* is limited to nine species only, two of which are calcicolous species associated to the concrete integration on a side of the object. Unfortunately, the quality of historic images of the *dolium* before its entry to the museum (see Mazzotti et al., 2021) did not allow to recognize if the other detected species may be remnants of a previous colonization, although the fact that the *dolium* had been thereafter cleaned cannot be ruled out. Oppositely, the higher proximity of the small *dolia* to the grass and the higher porosity determine a higher bioreceptivity, causing the quite complete lichen cover observed above the major curvature and the dominance of nitrophytic species, as *Protoparmeliopsis muralis*, *Flavoplaca* gr. *citrina* and *Verrucaria nigrescens* (while the presence of foliose Physciaceae is likely related to the presence of a tree in the nearby of the *dolia*). Differences in bioreceptivity seem to prevail rather than the period of permanence outdoors of the different *dolia*. The archival documentation (Mazzotti et al., 2021) reports that the big *dolium* had been located outdoors long before its arrival at the MIC. Afterwards, it was placed indoors from 1940 to 1950, then again outdoors until nowadays. Despite remaining outdoors for a much longer period than the other four *dolia*, which were positioned in the garden in the second half of the eighties in a cleaned state, the distribution of the colonization is very uneven.

As in the case of the big *dolium*, the low porosity of the sculptures is reflected by a sparser colonization in the case of Mazzini's work, mostly located in the horizontal areas more favorable to water retention, or quite null in the case of Tsvini's work. The part of the terrace where this latter sculpture is located can be regarded as an ecological micro-niche for its peculiar environmental conditions. The combination of very high temperatures (reaching around 52 °C), strong solar irradiation and low relative humidity (av. 50.7 %) in summer contributes to creating a very harsh situation for microorganisms to grow. Mazzini's sculpture is in the same place too, but the environmental condition is mitigated by its geometrical configuration because parts of it, including the mentioned horizontal areas, are shaded by other parts (Fig. 1c). Although the relatively low number of considered objects and the different states of several variables considered for each of them prevent a statistical support, all these considerations agree with the important relationships of material properties -remarkably porosity- and "architectural" geometries to determine the microenvironmental conditions which contribute to make a substrate colonized after a certain period of surface exposition, or not (Sanmartín et al., 2021).

In this context, it is worth considering the thin black-gray layer extensively observed on the small *dolia* and on Mazzini's sculpture, formed by the thalli of *Verrucaria nigrescens* and *Acarospora gallica*, by primordia of other crustose unidentifiable species and by non-lichenized black fungi 'parasitizing' the thalli and widely causing their disappearing. It is a peculiar pattern of biofilm-like lithobiontic colonization that, at the best of our knowledge, has not been described in other papers dealing with heritage stone objects, although it may have some implications for conservation issues. The fact that lichens can provide favorable microhabitats for the growth of other detriogenic lithobionts had been indeed demonstrated, but the phenomenon was mostly related to the cavities determined by the hyphal penetration, particularly in calcareous rocks (De Los Rios et al., 2002; Sohrabi et al., 2017). On the other hand, the thalline biomass is now widely accepted as a cradle of biodiversity, with the main symbiotic partners (mycobiont and photobiont) more or less strictly associated with bacteria (bacteriobionts) and additional fungal partners (Hawksworth and

Grube, 2020). These latter, i.e. the lichen mycobiome, include the asymptomatic endolichenic fungi, which are related to fungal endophytes of plants, and the symptomatic lichenicolous fungi, for which the literature reports a commensal to mildly parasitic lifestyle in the host thallus but, usually, not the observed aggressive behavior (see review in Grube and Muggia, 2021). Only a few lichenicolous species produce extensive damage, causing deactivation and decay of the host structures (Diederich et al., 2018; see review in Grube and Muggia, 2021). A particular feature of the *dolia*'s fungi relates to the fact that they colonize and parasitize only the lichens *Verrucaria nigrescens* and *Acarospora gallica* while do not develop at all on thalli of other species that grow close to them. In the case of *V. nigrescens*, this peculiar trait may be explained by the absence of secondary metabolic substances (Nimis, 2022), which in other species exert an allelopathic function against rock fungi (Gazzano et al., 2013) and may thus possibly regulate their overgrowth. However, *A. gallica* produces gyrophoric and lecanoric acid, so that factors other than the absence of secondary metabolites would also contribute to the observed differential susceptibility to fungal overgrowth.

Higher number of reads attributable to non-lichenized rock-inhabiting fungi was just obtained from *dolium* inv. 19074, on which the biofilm of meristematic fungi overgrowing *V. nigrescens* was prominent, while the sequences attributable to the lichen hosts prevailed in the other metabarcoding analyses related to the big *dolium* and Mazzini's statue. Fungal diversity recognized on the examined ceramic objects agrees with that reported on other monumental rock surfaces, with dominance of the orders Chaetothyriales, Capnodiales, and Pleosporales of Dothideomycetes (Onofri et al., 2014). This class is considered very diverse in terms of species, also including several plant pathogens, and epiphytes and rocks colonizers. Its component of rock inhabiting Dothideomycetes has been suggested as terroirs/refuges for plant associated fungi (Ruibal et al., 2009). Among the fungal genera found on *dolia* inv. 19074 and, at a lesser extent, inv. 10366,1 there are *Cladophialophora* and *Coniosporium/Knufia* (Chaetothyriales). They have been frequently found in different lichen hosts that, though, lacked any pathogenic symptoms (see review in Grube and Muggia, 2021). Other identified genera on the *dolia* and on Mazzini's sculpture surfaces were *Exophiala* (Chaetothyriales) and *Devriesia* (Capnodiales - this last was the only genus present on the sculpture). Fungi belonging to these genera are known as microcolonial fungi, characterized by meristematic and/or yeast growth as stress tolerant forms (Ruibal et al., 2009; Onofri et al., 2014), although their production of explorative thin hyphae has been also observed (Tonon et al., 2022 with refs. therein). All the genera have been frequently found on stone monuments in urbanized areas and on natural crops (Onofri et al., 2014; Isola et al., 2022). They can thrive under extreme conditions including irradiation, temperature, salinity, pH, and moisture (Coleine and Selbmann, 2021). They are stress-tolerant colonizers involved in biodeterioration of stone heritage (Sterflinger, 2010; Isola et al., 2016, 2022). Regarding the *dolia*, the hyphae of meristematic fungi developed isolated or as aggregates well beyond the lichen thalline biomass, and penetrated within the substrate, often arranged in clumps. In vitro experiments demonstrated that *Coniosporium/Knufia* species are able to produce chelating compounds and acids, and to lower the culture media pH, while *Exophiala* species do not (Favero Longo et al., 2011; Isola et al., 2022). Therefore, although the limited sample set of metabarcoding analyses likely did not allow an exhaustive characterization of the fungal diversity on the *dolia*, nevertheless it was sufficient to detect several fungi which could physically and/or chemically affect the ceramic substrate of MIC artworks. In the terrace corner hosting Tsvini's statue, even black fungi seemed to not endure the stressful microniche. Only a few dark-pigmented hyphae of *Cladosporium* species were found on the surfaces hosting the few sparse very little thalli of *Acarospora gallica*. The limited lichen colonization and the absence of other sources of organic matter in the protected terrace may be the factor limiting meristematic fungi, even though nutrients (milk and paraffin) could be potentially present in the substrate itself.

On *dolium* inv. 10366,1 a different biofilm was also observable. It covered a wide surface and was formed by an external layer of green algae and by

colonies of black meristematic fungi arranged in clumps just below the surface. Some of these fungi are likely belonging to genera growing on *dolium* inv. 19074 as it shares 10 % of fungal species with inv. 10366,1. As in the case of lichens, differences in dimension and geometry of the object, its intrinsic physico-chemical properties (porosity, chemistry and mineralogical composition), and conservation history likely explain the diverse colonization.

Bacterial communities associated to the lichen thalli show a composition compatible with those reported in other studies, with a predominance of Alphaproteobacteria and subordinate Actinobacteria and Betaproteobacteria (e.g. Aschenbrenner et al., 2016). In general, their presence seems less involved in biodeterioration patterns.

#### 4.3. Damaging and protective effects of the black-gray layer, algal biofilms and lichens on the substrates

The bio-weathering of *dolia*'s terracotta was related primarily to the black-gray layer formed by black meristematic fungi and the lichens *Verrucaria nigrescens* and *Acarospora gallica*. A dense network of hyphae belonging either to the lichens or to the fungi developed inside the substrate down to 2 mm. Although the thallus of *Verrucaria nigrescens* was thin, it included fragments of the substrate in it. Its hyphae were found in high amounts inside the substrate at more than 1 mm from the surface, in agreement with previous observations on ceramic tiles (Kiurski et al., 2005) and sandstone (Tonon et al., 2022). The other lichens (*Protoparmeliopsis muralis*, *Lecanora campestris* and *Lecidea fuscoatra*) mostly showed a lower hyphal penetration, down to 400  $\mu\text{m}$  or less. Some of these results have been confirmed by the measurement of stone surface hardness (Fig. 6) and of  $W_a$  values after the removal of the lithobiontic coverage (Table 3). The surface hardness values of terracotta under *Protoparmeliopsis muralis* were similar to those of the uncolonized substrate, thus demonstrating that this lichen developed mainly on the surface, while *Verrucaria nigrescens* penetrated the terracotta's bulk as the substrate values under it were much lower than those of the uncolonized areas, as reported on sandstone (Tonon et al., 2022) and limestone (Morando et al., 2017). These results have confirmed that the technique is a useful and suitable tool to measure the hardness of biodeteriorated surfaces, also in the case of ceramic objects. The highest values of  $W_a$  after the lithobiontic removal detected in the spots previously colonized by the black-gray layer of the fungal biofilm associated with *V. nigrescens* similarly confirm a biophysical effect negatively affecting the surface durability. On the contrary, the removal of the continuous lichen mosaic of the less penetrating species exposed surfaces with the lowest  $W_a$ , suggesting some bioprotection likely due to an umbrella-like sheltering effect.

Regarding water absorption before the removal of lithobionts, areas continuously covered by less penetrating epilithic crustose lichens and those colonized by the black-gray layer absorbed less water than uncolonized areas in all the monitoring measurements (Table 3). The result was noticeable in the small *dolia* inv. 19074 and 19075 while in the big *dolium* inv. 19066,1 the difference between colonized and uncolonized areas was not that high. This can be due to pores' diameters of the terracotta. Inv. 10366,1 presents a quite high frequency of pores with diameters ranging 5–100  $\mu\text{m}$ , while most pores of the other two *dolia* range 0.1–0.7  $\mu\text{m}$ . The total open porosity of inv. 19074 and 19075 is higher than that of inv. 10366,1, 36–41 % and 28.65 %, respectively. This physical characteristic accounted for the much higher water absorption of uncolonized areas of inv. 19074 and 19075 in comparison to inv. 10366,1. Nonetheless, the reduced amount of water absorbed by colonized areas was much notable in small *dolia*. This is likely due to the continuous lichen covering of small pores while the covering of big pores of inv. 10366,1 is not so continuous. Quite the same happened when the substrate was covered by thick black-gray layers, though with a slight increase of water absorbed, likely because the layers were not continuous. On the contrary, the thin green-black biofilm on inv. 10366,1 absorbed a higher amount of water than the uncolonized areas. The results of measurements performed on colonized surfaces indicated that lichens on ceramics with high total porosity and pores with very small diameters are able to reduce the amount of absorbed water limiting the water ingress. Accordingly,

limestone surfaces covered by lichens, including *V. nigrescens*, showed lower values of water absorption before the mechanical removal of thalli (Morando et al., 2017). On substrates having pores with big diameters, the effect is reduced even though it is almost the same. Regarding biofilms, their barrier efficacy relates to their thickness and composition. In particular, the algal biofilm on the big *dolium* impacts negatively on substrates enhancing the water absorption in comparison to uncolonized parts, likely because of the association with black fungi.

Regarding the hypothesis of potential positive effects of biological colonization on ceramics, the study thus showed a heterogeneous balance between biodeterioration and bioprotection for the different lithobionts, with some results being particularly worth of mentioning. First, poorly penetrating lichens did not influence surface hardness and contributed to reducing water absorption either when they colonized the stone or even after their removal. Second, the balance was in the direction of biodeterioration in the case of *Verrucaria nigrescens*, the black-gray layer deriving from its overgrowth by a fungal biofilm, and the green-black biofilm on the big *dolium*. Therefore, the equilibrium between biodeteriorative and bioprotective action of lichens is species-specific. Third, the bioprotection and biodeterioration of the examined lithobionts has been discussed for ceramics located in temperate areas, but equilibria may change in other climatic conditions.

## 5. Conclusions

This paper has analyzed and identified the lichen and microbial diversity on ceramics with different composition, structures and porosity. The biological colonization depended on these physical properties, on stone surface geometries as well as on climatic conditions of environments in which the ceramics artworks are located. An interesting result regarded the overgrowth of black meristematic fungi on two lichen species, *Acarospora gallica* and *Verrucaria nigrescens*, a process that ended up in the deactivation and disappearance of the lichens.

The results demonstrated that certain lichen species (*P. muralis*, *L. campestris*) may have a bioprotective effect on ceramics with high total porosity and pores with very small diameters as they poorly penetrate the substrate, do not negatively affect surface hardness and are able to reduce the amount of absorbed water limiting its ingress. By contrast, another species (*V. nigrescens*), here widely found in association with rock-dwelling fungi, deeply penetrates terracotta and is confirmed as agent of substrate disaggregation, with negative consequences on surface hardness and  $W_a$ , becoming operational after the removal of the biomass. Accordingly, a careful evaluation of the negative vs positive effects of lichen communities must be carried out before deciding their removal from an artwork. Regarding biofilms, their barrier efficacy is related to their thickness and composition. Even if thin, they can impact negatively on substrates enhancing the water absorption in comparison to uncolonized parts. However, it would be possible that the higher amount of water adsorbed by the biofilms is also caused by their water-retain properties. Therefore, water can be partially kept inside the biofilms and does not completely enter the ceramic. This hypothesis will be evaluated by further research.

Supplementary data to this article can be found online at <https://doi.org/10.1016/j.scitotenv.2023.162607>.

## CRedit authorship contribution statement

D. Pinna and S.E. Favero Longo conceived of the presented idea and wrote the manuscript with support from S. Gualtieri, V. Mazzotti, S. Voyron and A. Andreotti. D.P. supervised the project. All authors discussed the results and contributed to the final manuscript. All authors provided critical feedback and helped shape the research, analysis and manuscript.

## Data availability

No data was used for the research described in the article.

## Declaration of competing interest

I have nothing to declare.

## Acknowledgements

We are grateful to Elena Dal Prato, Federica Fanti and Paola Rondelli (MIC) for the assessment of the general state of preservation of the *dolia*, the collection and processing of T and RH data, and for the collaboration on tests with contact sponge.

## References

- Abarenkov, K., Zirk, A., Piirmann, T., Pöhönen, R., Ivanov, F., Nilsson, R.H., Kõljalg, U., 2021. UNITE QIIME Release for Fungi. Version 10.05.2021. UNITE Community <https://doi.org/10.15156/BIO/1264708>.
- Allen, J.L., Lendemer, J.C., 2022. A call to reconceptualize lichen symbioses. *Trends Ecol. Evol.* 37, 582–589.
- Amoros, L., Beltran, V., Escardino, A., Ortiz, M.J., 1992. Permeabilidad al aire de soportes cocidos de pavimento cerámico. I. Influencia de las variables de prensado y de la temperatura de cocción. *Bol. Soc. Esp. Ceram. Vidr.* 31 (1), 33–38.
- Anovitz, L., Cole, D., 2015. Characterization and analysis of porosity and pore structures. In: Steefel, C., Emmanuel, S., Anovitz, L. (Eds.), *Pore Scale Geochemical Processes*. Walter de Gruyter GmbH & Co KG, pp. 61–164.
- Apprill, A., McNally, S., Parsons, R., Weber, L., 2015. Minor revision to V4 region SSU rRNA 806R gene primer greatly increases detection of SARI1 bacterioplankton. *Aquat. Microb. Ecol.* 75, 129–137.
- Aschenbrenner, I.A., Cernava, T., Berg, G., Grube, M., 2016. Understanding microbial multi-species symbioses. *Front. Microbiol.* 7, 180.
- Bokulich, N.A., Kaehler, B.D., Rideout, J.R., Dillon, M., Bolyen, E., Knight, R., Huttley, G.A., Caporaso, J.G., 2018. Optimizing taxonomic classification of marker-gene amplicon sequences with QIIME 2's q2-feature-classifier plugin. *Microbiome* 6, 90.
- Bolyen, E., Rideout, J.R., Dillon, M.R., Bokulich, N.A., Abnet, C.C., Al-Ghalith, G.A., Alexander, H., Alm, E.J., Arumugam, M., Asnicar, F., et al., 2019. Reproducible, interactive, scalable and extensible microbiome data science using QIIME 2. *Nat. Biotechnol.* 37, 852–857.
- Bonaduce, I., Andreotti, A., 2009. Py-GC-MS of organic paint binders. In: Colombini, M.P., Modugno, F. (Eds.), *Organic Mass Spectrometry in Art And Archaeology*, Research Signpost. Wiley, UK, pp. 304–326.
- Bungartz, F., Garvie, L.A., Nash III, T., 2004. Anatomy of the endolithic Sonoran Desert lichen *Verrucaria rubrocincta* Breuss: implications for biodeterioration and biomineralization. *Lichenologist* 36, 55–73.
- Callahan, B.J., McMurdie, P.J., Rosen, M.J., Han, A.W., Johnson, A.J.A., Holmes, S.P., 2016. DADA2: high-resolution sample inference from Illumina amplicon data. *Nat. Methods* 13, 581–583.
- Carr, E.C., Harris, S.D., Herr, J.R., Riekhof, W.R., 2021. Lichens and biofilms: common collective growth imparts similar developmental strategies. *Algal Res.* 54, 102217.
- Carter, N.E.A., Viles, H.A., 2005. Bioprotection explored: the story of a little known earth surface process. *Geomorphology* 67, 273–281.
- Clauzade, G., Roux, C., 1985. Likenoj de Okcidenta Europo. *Ilustrita determinlibro*. Bull. Soc. Bot. Centre-Ouest, N. Ser., N. Spec. 7.
- Coleine, C., Selbmann, L., 2021. Black fungi inhabiting rock surfaces. In: Büdel, B., Thomas Friedl, T. (Eds.), *Life at Rock Surfaces Challenged by Extreme Light, Temperature And Hydration Fluctuations*. Walter de Gruyter GmbH, Berlin/Boston, pp. 57–77.
- Coletti, C., Cultrone, G., Maritan, L., Mazzoli, C., 2016. Combined multi-analytical approach for study of pore system in bricks: how much porosity is there? *Mater. Charact.* 121, 82–92.
- Coutinho, M.L., Miller, A.Z., Macedo, M.F., 2015. Biological colonization and biodeterioration of architectural ceramic materials: an overview. *J. Cult. Herit.* 16 (5), 759–777.
- Cultrone, G., Sebastián, V., Elerta, K., de la Torre, M.J., Cazalla, V., Rodríguez-Navarro, C., 2004. Influence of mineralogy and firing temperature on the porosity of bricks. *J. Eur. Ceram. Soc.* 24, 547–564.
- De Los Rios, A., Wierzbos, J., Ascaso, C., 2002. Microhabitats and chemical microenvironments under saxicolous lichens growing on granite. *Microb. Ecol.* 43, 181–188.
- Di Bella, M., Mazzoleni, P., Russo, S., Sabatino, G., Tigano, G., Tripodo, A., 2016. Archaeometric characterization of Roman volcanic millstones from Messina territory (Sicily, Italy). *Period. Mineral.* 85, 69–81.
- Diederich, P., Lawrey, J.D., Ertz, D., 2018. The 2018 classification and checklist of lichenicolous fungi, with 2000 non-lichenized, obligately lichenicolous taxa. *Bryologist* 121, 340–425.
- EN 17655, 2021. Conservation of Cultural Heritage - Determination of Water Absorption by Contact Sponge Method.
- Fabbri, D., Chiavari, G., 2001. Analytical pyrolysis of carbohydrates in the presence of hexamethyldisilazane. *Anal. Chim. Acta* 449, 271–280.
- Favero Longo, S.E., Gazzano, C., Giralda, M., Castelli, D., Tretiach, M., Baiocchi, C., Piervittori, R., 2011. Physical and chemical deterioration of silicate and carbonate rocks by meristematic microcolonial fungi and endolithic lichens (Chaetothyriomycetidae). *Geomicrobiol. J.* 28, 732–744.
- Favero-Longo, S.E., Viles, H.A., 2020. A review of the nature, role and control of lithobionts on stone cultural heritage: weighing-up and managing biodeterioration and bioprotection. *World J. Microbiol. Biotechnol.* 36 (7), 1–18.
- Flemming, H.C., Neu, T.R., Wozniak, D.J., 2007. The EPS matrix: the “house of biofilm cells”. *J. Bacteriol.* 189, 7945–7947.
- Flemming, H.C., Wingender, J., Szewzyk, U., Steinberg, P., Rice, S.A., Kjelleberg, S., 2016. Biofilms: an emergent form of bacterial life. *Nat. Rev. Microbiol.* 14, 563–575.
- Fomina, M., Skorochod, I., 2020. Microbial interaction with clay minerals and its environmental and biotechnological implications. *Minerals* 10, 861.
- Franco, C., Capelli, C., 2014. New archaeological and archaeometric data on Sicilian wine amphorae in the Roman period (1st to 6th Century AD). *Rei Cretariae Romanae Fautorum Acta* 43 554–547.
- Gazulla, M.F., Sánchez, E., González, J.M., Portillo, M.C., Orduna, M., 2011. Relationship between certain ceramic roofing tile characteristics and biodeterioration. *J. Eur. Ceram. Soc.* 31, 2753–2761.
- Gazzano, C., Favero-Longo, S.E., Iacomussi, P., Piervittori, R., 2013. Biocidal effect of lichen secondary metabolites against rock-dwelling microcolonial fungi, cyanobacteria and green algae. *Int. Biodeter. Biodegrad.* 84, 300–306.
- Gliozzo, E., 2020. Ceramic technology. How to reconstruct the firing process. *Archaeol. Anthropol. Sci.* 12, 260.
- Gliozzo, E., Turchiano, M., Fantozzi, P.L., Romano, A.V., 2018. Geosources for ceramic production and communication pathways: the exchange network and the scale of chemical representative differences. *Appl. Clay Sci.* 161, 242–255.
- Gliozzo, E., Goffredo, R., Totten, D.M., 2019. Painted and common wares from Salapia (Cerignola, Italy): archaeometric data from fourth to eighth centuries AD samples from the Apulian coast. *Archaeol. Anthropol. Sci.* 11, 2659–2681.
- Gorbushina, A., Broughton, W.J., 2009. Microbiology of the atmosphere-rock interface: how biological interactions and physical stresses modulate a sophisticated microbial ecosystem. *Annu. Rev. Microbiol.* 63, 431–450.
- Grube, M., Muggia, L., 2021. Complex lichen communities inhabiting rock surfaces. In: Büdel, B., Friedl, T. (Eds.), *Life at Rock Surfaces Challenged by Extreme Light, Temperature And Hydration Fluctuations*. Walter de Gruyter GmbH, Berlin/Boston, pp. 175–185.
- Guamet, P.S., Sotoc, D.M., Schultz, M., 2019. Bioreceptivity of archaeological ceramics in an arid region of northern Argentina. *Int. Biodeterior. Biodegrad.* 141, 2–9.
- Guillitte, O., 1995. Bioreceptivity: a new concept for building ecological studies. *Sci. Total Environ.* 167, 215–220.
- Hawksworth, D.L., Grube, M., 2020. Lichens redefined as complex ecosystems. *New Phytol.* 227 (5), 1281–1283.
- Honegger, R., 2012. The symbiotic phenotype of lichen-forming ascomycetes and their endo- and epibionts. In: Hock, B. (Ed.), *Fungal Associations*. Springer, Berlin, Heidelberg, pp. 287–339.
- Ihrmark, K., Bodeker, I.T., Cruz-Martinez, K., Friberg, H., Kubartova, A., Schenck, J., Strid, Y., Stenlid, J., Brandström-Durling, M., Clemmensen, K.E., Lindahl, B.D., 2012. New primers to amplify the fungal ITS2 region - evaluation by 454-sequencing of artificial and natural communities. *FEMS Microbiol. Ecol.* 82, 666–677.
- Isola, D., Zucconi, L., Onofri, S., Caneva, G., De Hoog, G.S., Selbmann, L., 2016. Extremotolerant rock inhabiting black fungi from Italian monumental sites. *Fungal Divers.* 76 (1), 75–96.
- Isola, D., Bartoli, F., Meloni, P., Caneva, G., Zucconi, L., 2022. Black fungi and stone heritage conservation: ecological and metabolic assays for evaluating colonization potential and responses to traditional biocides. *Appl. Sci.* 12, 2038.
- Jordan, M.M., Montero, M.A., Meseguer, S., Sanfeliu, T., 2008. Influence of firing temperature and mineralogical composition on bending strength and porosity of ceramic tile bodies. *Appl. Clay Sci.* 42, 266–271.
- Kiurski, J.S., Ranogajec, J.G., Ujhelji, A.L., Radeka, M.M., Bokorov, M.T., 2005. Evaluation of the effect of lichens on ceramic roofing tiles by scanning electron microscopy and energy-dispersive spectroscopy analyses. *Scanning* 27 (3), 113–119.
- Laiz, L.L., González, J.M., Saiz-Jiménez, C., Portillo, M.C., Gazulla, M.F., Sánchez, E., 2006. Microbial assessment of the biological colonization on roofing tiles. In: Fort, R., Álvarez de Burgo, M., Gómez-Heras, M., Vázquez-Calvo, C. (Eds.), *Heritage, Weathering And Conservation*. Taylor & Francis, London, pp. 349–353.
- Liu, X., Koestler, R.J., Warscheid, T., Katayama, Y., Gu, J.D., 2020. Microbial deterioration and sustainable conservation of stone monuments and buildings. *Nat. Sustain.* 3, 991–1004.
- Liu, X., Qian, Y., Wu, F., Wang, Y., Wang, W., Gu, J.D., 2022. Biofilms on stone monuments: biodeterioration or bioprotection? *Trends Microbiol.* 30, 816–819.
- de los Rios, A., Cámara, B., García del Cura, M.A., Rico, V.J., Galván, V., Ascaso, C., 2009. Deteriorating effects of lichen and microbial colonization of carbonate building rocks in the Romanesque Churches of Segovia (Spain). *Sci. Total Environ.* 407 (3), 1123–1134.
- Maritan, L., 2020. Ceramic abandonment. How to recognise post-depositional transformations. *Archaeol. Anthropol. Sci.* 12, 199.
- Mazzotti, V., Rondelli, P., Gualtieri, S., Pinna, D., Magrini, D., 2021. I dolia nel giardino del MIC di Faenza: studio diagnostico per il restauro. Proceedings of the conference La Conservazione della Ceramica all'Aperto, Faenza, Italy, pp. 9–21.
- McIlroy de la Rosa, J.P.M., Warke, P.A., Smith, B.J., 2013. Lichen-induced biomodification of calcareous surfaces: bioprotection versus biodeterioration. *Prog. Phys. Geogr.* 37, 325–351.
- Miller, A.Z., Dionísio, A., Sequeira Braga, M.A., Hernández-Mariné, M., Afonso, M.J., Muralha, V.S.F., Herrera, L.K., Raabe, J., Fernandez-Cortes, A., Cuezva, S., Hermosin, B., Sanchez-Moral, S., Chaminé, H., Sáiz-Jiménez, C., 2012. Biogenic Mn oxide minerals coating in a subsurface granite environment. *Chem. Geol.* 322–323, 181–191.
- Morando, M., Wilhelm, K., Matteucci, E., Martire, L., Piervittori, R., Viles, H.A., Favero Longo, S.E., 2017. The influence of structural organization of epilithic and endolithic lichens on limestone weathering. *Earth Surf. Process. Landf.* 42 (11), 1666–1679.
- Naylor, L.A., Viles, H.A., Carter, N.E.A., 2002. Biogeomorphology revisited: looking towards the future. *Geomorphology* 47, 3–14.
- Nimis, P.L., 2016. *The Lichens of Italy. A Second Annotated Catalogue*. Edizioni Università di Trieste, Italy.
- Nimis, P.L., 2022. ITALIC - The information system on italian lichens. Version 7.0. University of Trieste, Dept. of Biology accessed on 2022, 07, 14. All data are released under a CC BY-SA 4.0 license <https://dryades.units.it/italic>.

- Nimis, P.L., Martellos, S., 2020. Towards a digital key to the lichens of Italy. *Symbiosis* 82 (1), 149–155.
- Nimis, P.L., Pinna, D., Salvadori, O., 1992. *Licheni e conservazione dei monumenti*. Cooperativa Libreria Universitaria Editrice, Bologna, Italy.
- Omelon, C.R., 2016. Endolithic microorganisms and their habitats. In: Hurst, C.J. (Ed.), *Advances in Environmental Microbiology. Their World: A Diversity of Microbial Environments*. Springer, Cincinnati, USA, pp. 171–201.
- Onofri, S., Zucconi, L., Isola, D., Selbmann, L., 2014. Rock-inhabiting fungi and their role in deterioration of stone monuments in the Mediterranean area. *Plant Biosyst.* 148 (2), 384–391.
- Osrini, S., Parlanti, F., Bonaduce, I., 2017. Analytical pyrolysis of proteins in samples from arctic and archaeological objects. *J. Anal. Appl. Pyrolysis* 124, 643–657.
- Pena-Poza, J., Ascaso, C., Sanz, M., Pérez-Ortega, S., Oujja, M., Wierzchos, J., Souza-Egipsy, V., Cañameres, M.V., Urizal, M., Castillejo, M., García-Heras, M., 2018. Effect of biological colonization on ceramic roofing tiles by lichens and a combined laser and biocide procedure for its removal. *Int. Biodeterior. Biodegrad.* 126, 86–94.
- Pesaresi, S., Biondi, E., Casavecchia, S., 2017. Bioclimates of Italy. *J. Maps* 13, 955–960.
- Pinna, D., 2014. Biofilms and lichens on stone monuments: do they damage or protect? *Front. Microbiol.* 5, 1–3.
- Pinna, D., 2021. Microbial growth and its effects on inorganic heritage materials. In: Joseph, E. (Ed.), *Microorganisms in the Deterioration And Preservation of Cultural Heritage*. Springer, pp. 3–36.
- Quagliarini, E., Gianangeli, A., D'Orazio, M., Gregorini, B., Osimani, A., Aquilanti, L., Clementi, F., 2019. Effect of temperature and relative humidity on algae biofouling on different fired brick surfaces. *Constr. Build. Mater.* 199, 396–405.
- Radeka, M., Ranogajec, J., Kiurski, J., Markov, S., Marinković-Nedučin, R., 2007. Influence of lichen biocorrosion on the quality of ceramic roofing tiles. *J. Eur. Ceram. Soc.* 27 (2–3), 1763–1766.
- Ricciardi, P., Nodari, L., Fabbri, B., Gualtieri, S., Russo, U., 2007. Contribution for a mineral-ogical thermometer to be applied to low fired and/or non-carbonate ceramics. *Proc. EMAC '05, 8th European Meeting on Ancient Ceramics, Lyon, BAR International Series 1691*, pp. 13–18.
- Robeson II, M.S., O'Rourke, D.R., Kaehler, B.D., Ziemski, M., Dillon, M.R., Foster, J.T., Bokulich, N.A., 2021. REScript: reproducible sequence taxonomy reference database management. *PLoS Comput. Biol.* 17 (11), e1009581.
- Ruibal, C., Gueidan, C., Selbmann, L., Gorbushina, A.A., Crous, P.W., Groenewald, J.Z., Muggia, L., Grube, M., Isola, D., Schoch, C.L., Staley, J.T., Lutzoni, F., de Hoog, G.S., 2009. Phylogeny of rock-inhabiting fungi related to Dothideomycetes. *Stud. Mycol.* 64, 123–133.
- Salvadori, O., Casanova, A., 2016. The role of fungi and lichens in the biodeterioration of stone monuments. *Open Conf. Proc. J.* 7, 39–54.
- Sanmartín, P., Miller, A.Z., Prieto, B., Viles, H.A., 2021. Revisiting and reanalysing the concept of bioreceptivity 25 years on. *Sci. Total Environ.* 770, 145314.
- Seaward, M.R.D., 1997. Major impacts made by lichens in biodeterioration processes. *Int. Biodeterior. Biodegrad.* 40 (2–4), 269–273.
- Seaward, M.R.D., 2004. Lichens as subversive agents of biodeterioration. In: Seaward, M.R.D., St. Clair, L.L. (Eds.), *Biodeterioration of Stone Surfaces*. Springer, Dordrecht, pp. 9–18.
- Sohrabi, M., Favero-Longo, S.E., Perez-Ortega, S., Ascaso, C., Haghghat, Z., Hassan Talebian, M., Fadaei, H., de los Ríos, A., 2017. Lichen colonization and associated deterioration processes in Pasargadae, UNESCO world heritage site, Iran. *Int. Biodeterior. Biodegrad.* 117, 171–182.
- Spribile, T., Resl, P., Stanton, D.E., Tagirdzhanova, G., 2022. Evolutionary biology of lichen symbioses. *New Phytol.* 234 (5), 1566–1582.
- Sterflinger, K., 2010. Fungi: their role in deterioration of cultural heritage. *Fungal Biol. Rev.* 24, 47–55.
- Takahashi, S., Tomita, J., Nishioka, K., Hisada, T., Nishijima, M., 2014. Development of a prokaryotic universal primer for simultaneous analysis of bacteria and archaea using next-generation sequencing. *PLoS ONE* 9 (8), e105592.
- Tonon, C., Bernasconi, D., Martire, L., Pastero, L., Viles, H., Favero-Longo, S.E., 2022. Lichen impact on sandstone hardness is species - specific. *Earth Surf. Process. Landf.* 47 (5), 1147–1156.
- Tschegg, C., 2009. Post-depositional surface whitening of ceramic artifacts: alteration mechanisms and consequences. *J. Archaeol. Sci.* 36, 2155–2161.
- Urzi, C., Bruno, L., De Leo, F., 2018. Biodeterioration of paintings in caves, catacombs and other hypogean sites. In: Mitchell, R., Clifford, J. (Eds.), *Biodeterioration And Preservation in Art, Archaeology And Architecture*. Archetype Publications Ltd, pp. 114–129.
- White, T.J., Bruns, T., Lee, S., Taylor, J., 1990. Amplification and direct sequencing of fungal ribosomal RNA genes for phylogenetics. In: Innis, M., Gelfand, D., Sninsky, J., White, T. (Eds.), *PCR Protocols: A Guide to Methods And Applications*. Academic Press Inc., New York, USA, p. 315.
- Whitlatch, R.B., Johnson, R.G., 1974. Methods for staining organic matter in marine sediments. *J. Sediment. Petrol.* 44, 310–312.
- Wilhelm, K., Viles, H., Burke, O., Mayaud, J., 2016. Surface hardness as a proxy for weathering behaviour of limestone heritage: a case study on dated headstones on the Isle of Portland, UK. *Environ. Earth Sci.* 75, 1–16.